Mitigating Emissions and Energy Consumption for Urban Transportation Networks: Simulation-Based Signal Control Strategies

by

Kanchana Nanduri

B.Tech in Civil Engineering
Indian Institute of Technology Mumbai, 2011

Submitted to the Department of Civil and Environmental Engineering
in partial fulfillment of the requirements for the degree of

Master of Science in Transportation

at the

MASSACHUSETTS INSTITUTE OF TECHNOLOGY

June 2013

© Massachusetts Institute of Technology 2013. All rights reserved.

Author .....
Department of Civil and Environmental Engineering
May 24, 2013

Certified by .....
Carolina Osorio
Assistant Professor of Civil and Environmental Engineering
Thesis Supervisor

Accepted by .....
Heidi M. Nepf
Chair, Departmental Committee for Graduate Students

Mitigating Emissions and Energy Consumption for Urban Transportation Networks: Simulation-Based Signal Control Strategies

by

Kanchana Nanduri

Submitted to the Department of Civil and Environmental Engineering
on May 24, 2013, in partial fulfillment of the
requirements for the degree of
Master of Science in Transportation

Abstract

Microscopic urban traffic simulators embed the most detailed traveler behavior and network supply models. They represent individual vehicles and can therefore account for vehicle-specific technologies. These simulators can be coupled with instantaneous energy consumption and emissions models to yield detailed network-wide estimates of energy consumption and pollutant emissions. Nonetheless, there is currently a lack of computationally efficient optimization techniques that enable the use of these complex integrated models to design sustainable transportation strategies.

This thesis proposes a methodology that combines a stochastic microscopic traffic simulation model with an instantaneous vehicular fuel consumption model and consecutively, with an instantaneous vehicular emissions model. The combined models are embedded within a simulation-based optimization (SO) algorithm and used to address a signal control problem. First, a framework that combines travel time and fuel consumption in the objective is formulated followed by one combining travel time and various pollutant emissions. The proposed technique couples detailed, stochastic and computationally inefficient models, yet is an efficient optimization technique. Efficiency is achieved by combining simulated observations with analytical approximations of the objective functions.

This methodology is applied to a network within the Swiss city of Lausanne. The proposed method identifies signal plans with improved travel time, fuel consumption and emissions metrics, and does so within a tight computational budget. It systematically outperforms traditional techniques, particularly when performance metrics with high variance, such as fuel consumption and emissions, are used. This method enables the use of disaggregate instantaneous vehicle-specific information to inform and improve traffic operations at the network-scale.

Thesis Supervisor: Carolina Osorio
Title: Assistant Professor of Civil and Environmental Engineering

Acknowledgments

I would first like to thank my advisor, Prof. Carolina Osorio, for her encouragement and unwavering faith in our research goals. This thesis is as much her effort as it is mine. I consider my time at MIT to be one of the most productive periods in my life and she pushed me to keep busy while enjoying what I was doing. I would also like to thank Prof. Steven Barrett of the Department of Aeronautics and Astronautics at MIT, for his valuable inputs on emissions modeling in the field of transportation.

I would like to thank everyone in my office, 1-151. Carter, Jameson, Joel, Andres, Naomi, Carlos, Serdar, Ryan and Laura: thank you for always being there to lighten my mood. While our office had to be one of the most chaotic rooms I have ever been in, the knowledge that I would always have you guys by my side, on good days or bad, was a thought that helped me on countless occasions during my last two years at MIT. This thesis would never have been possible without you all. And finally, thank you Linsen for helping me debug so many codes. I will always owe you for that.

Last but not the least, I would like to thank my family for their love and reassuring phone-calls during the stressful period of thesis-writing. I am very lucky to have you all in my life.

Contents

List of Figures

Chapter 1

Introduction

The International Energy Agency (IEA, 2012) has estimated that over 50% of oil use worldwide is from transport and three-quarters of the energy used in the transport sector is consumed on the roads. The IEA also projects that without strong new measures, road transport energy use will double between 2010 and 2050. The energy consumed every day on our roads not only contributes to the depletion of a valuable natural resource but the linear relationship between fuel consumption and carbon dioxide (CO_2) emissions means that urban traffic plays a role in global warming. Apart from carbon dioxide emissions, urban traffic is also responsible for emissions of pollutants like nitrogen oxides (NO_x), volatile organic compounds (VOC) and particulate matter (PM). In a recent report published jointly by the World Health Organization and the Transport Policy Advisory Services of the German goverment (WHO and GIZ, 2011), it estimated that road transport contributes up to 30% of PM concentrations in European cities and up to 69% in cities of the developing world. The report also confirms that transport is a leading source of other air pollutants, including carbon monoxide (CO), oxides of nitrogen, as well as benzene (part of the volatile organic compound family) which causes formation of ground-level ozone also known as smog. It finds that transport-related air pollutants increase the risk of a number of health problems, including cardiovascular and respiratory disease, cancer and adverse birth outcomes, and are associated with higher death rates in populations exposed. Thus, there is a need to understand how the use of existing urban transportation

infrastructure can be enhanced to reduce energy consumption and urban traffic emissions. Signal control remains a viable solution in this regard: the re-timing effort involved is low-cost and the environmental benefits can be realized within a short time-span.

Over the past decade state-of-the-art traffic, fuel consumption and emissions simulators have been developed independently, coupled and extensively used to evaluate the impacts of various transportation projects on traffic, fuel consumption and emissions. Nonetheless, there is currently a lack of computationally efficient optimization techniques that enable the use of these complex integrated models to design sustainable transportation strategies.

This thesis proposes a methodology that combines detailed traffic and fuel consumption/emissions models, in order to design traffic signal control strategies that improve both traditional traffic metrics (e.g., average network travel times) as well as reduce total fuel consumption and emissions in the considered network. The main challenge is to use the most detailed and thus inherently inefficient models, while simultaneously deriving a computationally efficient methodology.

Traffic simulators can be primarily classified as macroscopic, mesoscopic or microscopic according to their modeling scale (for reviews see Barceló (2010), Boxill and Yu (2000), Algers et al. (1997)). Macroscopic simulators use models that describe the progression of traffic along links as a function of average link speed, flow and density. Macroscopic models are therefore flow-based models that provide an aggregate representation of traffic. Vehicles along a link are collectively represented. This leads to models that have few parameters to calibrate, are computationally efficient and well-suited to address large-scale networks. These advantages come at the cost of a non-detailed (aggregate) description of traffic.

Microscopic models represent each individual traveler and/or vehicle. Driver-specific attributes (e.g., socio-economic attributes) and vehicle-specific characteristics (e.g. vehicle type, vehicle technology) can be accounted for. They provide a highly detailed representation of network flows and use disaggregate behavioral models (e.g., departure-time choice, mode choice, lane changing, car-following) to describe the

reaction of individual drivers towards network components, traffic conditions and adjacent drivers. Such detail leads to data-intensive and computationally-intensive models. Mesoscopic traffic simulators lie on the spectrum between microscopic and macroscopic simulators.

Similarly, fuel consumption and emissions models can primarily be categorized as macroscopic or microscopic (for reviews see Rakha et al. (2003), Cappiello (2002), Williams and Yu (2001)). Macroscopic models estimate fuel consumption and emissions based on average speed/acceleration. However, both metrics are known to depend on the spatial-temporal variations of both speed and acceleration. Past work has, for instance, shown how different instantaneous profiles associated with different fuel consumption and emissions may lead to common average speed/acceleration profiles (Rakha et al., 2000). Microscopic models rely on instantaneous (e.g., second-by-second) speeds and accelerations of individual vehicles to estimate fuel consumption and emissions and are thus considered more accurate.

Integrating microscopic traffic models with microscopic fuel consumption/emissions models is particularly suitable when studying the impact of network changes on fuel consumption and emissions. While the traffic model accounts for the complex vehicle-to-vehicle and vehicle-to-supply interactions, the fuel consumption/emissions model gives detailed estimates of the fuel consumed and the different types of pollutants emitted, with the choice of various levels of aggregation from individual vehicles to network-level estimates. However, the detail of such integrated models comes with an increased computational evaluation cost, as well as a greater challenge to embed them within an optimization framework.

This thesis focuses on the development of computationally efficient simulation-based optimization (SO) techniques which account for environmental metrics such as fuel consumption and emissions in the objective and can yield solutions within a tight simulation budget (defined as a maximum number of simulation runs or run time). Such techniques respond to the needs of practitioners by allowing them to address real problems in a practical manner. In the remainder of this chapter, we present a brief description of the thesis structure. This thesis is organized as follows:

Chapter 2 describes the methodology used to incorporate fuel consumption within an SO framework and the application of this framework to a case study in Lausanne, a city in Switzerland. The empirical results obtained in this case study were presented at the 4th International Symposium on Dynamic Traffic Assignment (Osorio and Nanduri, 2012) and also submitted for journal publication.

Chapter 3 presents the formulation of the proposed SO algorithm when it is applied to address a traffic signal control problem accounting for emissions. Once again, results from a Lausanne city case study are analyzed. This chapter will also be submitted for journal publication.

Chapter 4 enumerates some conclusions summarizing the main ideas in the thesis and presents an outlook for future lines of research that can arise based on the results of this study.

Appendices. The appendices provide: A) the formulation of the analytical queueing network model used in this study, which was proposed by Osorio and Bierlaire (2009a and 2009b); B) Details regarding the formulation of the trust-region subproblem used to derive a trial point at each iteration of the SO algorithm proposed by Osorio and Bierlaire (2010).

Chapter 2

Energy-efficient signal control

2.1 Literature review

The interactions between traffic operations and fuel consumption have been extensively investigated over the past three decades, since the seminal work of Robertson (1983). In this section, we review recent work that has coupled traffic simulators with fuel consumption models to address urban transportation problems. For early references, we refer the reader to the review presented in Liao and Machemehl (1998).

Ikeda et al. (1999) modify the usual objective function (called the performance index) of the macroscopic TRANSYT (Robertson, 1969) signal control technique to explicitly account for fuel consumption. A case study considering a 10-link linear network in Yokohama, Japan, is carried out. Li et al. (2004) develop a macroscopic fuel consumption and emissions model that is combined with a macroscopic traffic model. The combined model is used to evaluate the impact of a set of predetermined cycle length values of a signal plan for one intersection in Nanjing, China.

Zegeye et al. (2010) couple the macroscopic traffic model METANET (Messmer and Papageorgiou, 1990) with a microscopic fuel consumption and emissions model VT-Micro (Rakha et al., 2004). As a macroscopic model, METANET provides only average link speeds and accelerations. These are plugged into VT-Micro (at every simulation step) as if they were instantaneous vehicle speeds. The combined models are embedded within a dynamic control framework. They consider a dynamic

speed limit problem along with an objective function that combines three metrics: total travel time, total fuel consumption and total CO_2 emissions. Their case study considers a hypothetical 12km 2-lane freeway.

Cappiello (2002) couples a mesoscopic traffic model (Bottom, 2000) with a microscopic fuel consumption and emissions model. They consider a hypothetical 14-link network, and evaluate the travel time and fuel consumption performance of a set of predetermined variable message sign strategies. Williams and Yu (2001) use the macroscopic traffic model DYNAMIC (Yu, 1994) along with a macroscopic fuel consumption model. They consider two hypothetical networks with, respectively, one and two signalized intersection(s) and evaluate the fuel consumption performance of several predetermined cycle lengths.

In order to provide a more accurate representation of the interaction between vehicular fuel consumption and supply changes, microscopic traffic and fuel consumption models have been coupled. Stathopoulos and Noland (2003) use the microscopic models VISSIM (PTV, 2008) and CMEM (Scora and Barth, 2006) albeit not in an optimization context. The coupled models are used to evaluate the travel time, fuel consumption and emissions impacts of a set of predetetermined scenarios for two hypothetical transportation projects (capacity expansion of an arterial bottleneck, synchronization of traffic signals) on a hypothetical linear network with three signalized intersections

Rakha et al. (2004) develop a microscopic fuel/emissions model known as VT-Micro. This model is used in Rakha et al. (2000) along with the microscopic simulator INTEGRATION (Van Aerde, 1999) to evaluate the performance of predetermined signal plans considering a linear network with four links and simple demand profiles.

To the best of our knowledge, the only work that has integrated microscopic traffic and fuel consumption models to perform optimization is that of Stevanovic et al. (2009). They integrate VISSIM (PTV, 2008) with CMEM (Scora and Barth, 2006), and embed the coupled models within the signal optimization tool VISGAOST (Stevanovic et al., 2008). Their case study considers a network of 2 arterials with 14 signalized intersections in Park City, Utah, USA. They investigate various formu-

lations of the signal control problem (e.g., objective functions consider throughput, stops, delay, fuel consumption or CO_2 emissions). Their problems have over 100 signal control variables. For each problem they run a total of 60,000 simulation runs (12,000 signal plans evaluated across 5 simulation replications each). This is a flexible approach, yet is not designed to address problems under tight computational budgets.

To summarize, traffic models coupled with fuel consumption models have been applied at macroscopic, mesoscopic and microscopic scales in traffic management. Microscopic simulators incorporate disaggregate behavioral models which make them ideal for scenario-based analysis and accurate estimation of network performance measures (such as fuel consumption and travel time).

However, the use of microscopic simulators coupled with detailed fuel consumption models has been mainly limited to evaluating the effect of a set of predetermined alternatives. This can primarily be attributed to the challenges faced when integrating microscopic simulators in an optimization framework. The outputs from the simulator are stochastic and non-linear with possibilities for numerous local minima. Also, a large number of replications are needed to derive accurate estimates of the objective function thus driving up computational costs.

In the next section, a simulation-based optimization technique is proposed that uses integrated microscopic traffic and fuel consumption models to address signal control problems. The SO technique can identify signal plans with improved performance within a limited computational budget, i.e. it is efficient. Additionally, we also illustrate how highly variable outputs from traffic simulators (e.g., fuel consumption) can be efficiently used for optimization purposes. This method enables the use of disaggregate instantaneous vehicle-specific information to inform and improve traffic operations at the network-scale.

2.2 Methodology

2.2.1 Simulation-based optimization framework

In this thesis we use the SO framework of Osorio and Bierlaire (2010). Hereafter, we refer to it as the *initial framework*. It allows for generally constrained continuous optimization problems. The constraints have analytical differentiable expressions, but there is no analytical expression of the objective function. The latter is defined implicitly by the simulator. Such problems can be formulated as:

$$\min_{x \in \Omega} g(x; p) \equiv E[G(x; p)], \tag{2.1}$$

where the objective function g is the expected value of a suitable stochastic network performance measure, G. It is a function of a deterministic continuous decision or control vector x and deterministic exogenous parameters p. The feasible space Ω consists of a set of general, typically non-convex, deterministic, analytical and differentiable constraints.

In a signal control problem x can represent the green times (or green splits) for the signalized lanes, whereas p accounts, for example, for the total demand or the network topology. Past work has used traditional performance measures, such as expected travel time (Osorio and Bierlaire, 2010, Osorio and Chong, 2012, Chen et al., 2012), as objective functions. This chapter considers a more challenging objective that accounts both for expected travel time and for expected fuel consumption which depends not only on traffic conditions but also on the underlying vehicle type and technology.

A given simulation run yields a realization of the random variable G. A given simulation run involves sampling for each vehicle (or traveler) from the numerous probability distributions that account for uncertainty in, for instance, traveler behavior (e.g., route choice for individual drivers) or traffic generation (e.g., headways of vehicles entering the network). For any network performance measure G, $E[G(x; p)]$ is an intricate function of x.

The SO approach used in this thesis, is based on a metamodel technique. We give an overview of its main ideas below. For details, we refer the reader to Osorio and Bierlaire (2010). Each iteration of the SO algorithm considers a given point x and proceeds through two main steps. Firstly, it collects a sample of simulated observations of $G(x;p)$ and estimates $g(x;p)$ by the sample average. The estimate is denoted $\hat{g}(x;p)$. This estimate along with estimates at other points in previous iterations, are used to fit an analytical approximation of the objective function. The latter is called the metamodel or surrogate model. Secondly, the metamodel is used to solve a signal control problem, and to derive a trial point (e.g., new signal plan).

The performance of the trial point is then evaluated with the simulator (first step), and the process iterates until the computational budget is depleted. This SO technique resorts to a derivative-free trust region algorithm, which is based on the algorithm of Conn et al. (2009). That is, at each iteration of the SO algorithm the trial point is derived by solving a trust region subproblem.

The most common choice of a metamodel are generic functions, such as polynomials. These are chosen for their analytical properties (e.g., they may asymptotically provide an excellent local fit), yet may not provide a good global approximation of the objective function. Additionally, their functional form is independent of the considered application or problem. The initial framework uses a metamodel that combines a generic component with what is known in the metamodeling field as a physical component. The latter is an application and problem-specific approximation of the objective function.

The metamodel has the following form:

$$m(x,y;\alpha,\beta,q) = \alpha g^A(x,y;q) + \phi(x;\beta), \tag{2.2}$$

where the following notation is used:

m	metamodel;
x	decision vector;
g^A	approximation of the objective function derived by the analytical model;
ϕ	polynomial quadratic in x with diagonal second derivative matrix;
y	endogenous queueing model variables;
q	exogenous queueing model parameters;
α, β	metamodel parameters.

The metamodel is a combination of a physical component g^A and a generic component ϕ. The physical component g^A is an analytical approximation of the objective function provided by a physical model (e.g. a macroscopic urban traffic model or a macroscopic fuel consumption model). For instance, the macroscopic traffic model used in this thesis is based on finite capacity queueing theory (more details on this model are given in Section 2.2.2). The physical component provides a global approximation of the objective function. Since it provides closed-form continuous expressions for the performance measures and their first-order derivatives, it surmounts the main limitations of the simulator; and thus leads to a computationally efficient SO algorithm. The parameters of the metamodel, α and β, are fitted by using the simulated observations and solving a least squares problem (see Osorio and Bierlaire (2010) for details).

Past work has considered traditional objective functions, mainly expected travel time, which can be relatively well approximated by macroscopic models. Nonetheless, the use of less traditional, as well as vehicle-technology dependent, objectives functions remains a challenge.

This chapter considers an objective functions that accounts for vehicle-specific fuel consumption in addition to travel time. This performance measure is highly dependent on both vehicle types, vehicle technologies and instantaneous vehicle accelerations and speeds, which have complex spatial-temporal variations in congested networks. We consider tight computational budgets (i.e., few simulation runs are

allowed), where deriving a suitable analytical approximation of the relationship between city-wide fuel consumption or emissions and signal plans is an even greater challenge.

2.2.2 Traffic Models

We use the same traffic models as in the initial framework.

Microscopic simulation model

We use a microscopic traffic simulation model of the Swiss city of Lausanne (Dumont and Bert, 2006). It is calibrated for evening peak period traffic. This model accounts for the behavior of individual drivers within the network. Trips are generated based on an origin-destination matrix, along with a headway model. Driver behavior is modeled using car following, lane changing, gap acceptance and route choice models. It is implemented with the Aimsun software (TSS, 2011).

Macroscopic analytical model

The analytical model combines ideas from finite capacity queueing theory, national transportation norms, and other urban traffic models. It models each lane of an urban network as a set of finite capacity queues. It is formulated as a system of nonlinear equations (its formulation is given in Appendix A). Its formulation is derived in Osorio and Bierlaire (2009b), which is based on the more general queueing network model of Osorio and Bierlaire (2009a). The model uses the finite capacity queueing theory notion of blocking to describe how congestion arises and propagates through the network. It analytically approximates how upstream and downstream queues interact.

2.2.3 Fuel consumption models

Microscopic simulation model

We use the microscopic fuel consumption model embedded in Aimsun (v6.1). This detailed model accounts for the time spent by each vehicle in the network during each simulation time-step in each of the four operating modes namely idling, deceleration, acceleration and cruising. The fuel consumed during the idling, deceleration and acceleration modes is derived from Ferreira (1982) (pages 4-16), while the fuel consumed during the cruising mode is derived from Akçelik (1983) (pages 51-53).

During a given simulation time-step the fuel consumed by a given vehicle j is given by:

$$FC_j = C_{1j}t_j^I + C_{2j}t_j^D + (C_{3j} + C_{4j}v_j a_j)t_j^A + [C_{5j}(1 + \frac{v_j^3}{2(V_j^m)^3}) + C_{6j}v_j]t_j^C, \quad (2.3)$$

where the following notation for a given vehicle j is used:

FC_j	fuel consumed during a given simulation time step (in mℓ);
C_{1j}	idling fuel consumption rate;
C_{2j}	decelerating fuel consumption rate;
C_{3j}, C_{4j}	accelerating mode constants;
C_{5j}, C_{6j}	cruising mode constants;
V_j^m	speed at which vehicle fuel consumption is minimum;
t_j^M	time spent in a given mode $M \in \{I$ (idling), D (deceleration), A (acceleration), C (cruising)$\}$;
v_j	instantaneous speed (in m/s);
a_j	instantaneous acceleration (in m/s^2).

In the right-hand side of Equation (2.3), capital letters are used to denote the exogenous vehicle-specific parameters. The simulation time step Δt is such that $\Delta t = t_j^I + t_j^D + t_j^A + t_j^C$. In the considered simulation, $\Delta t = 0.75$ seconds and the individual components t_j^I, t_j^D, t_j^A, t_j^C are determined by the microsimulator. The con-

stants C_{1j} to C_{6j} and V_j^m are provided by the vehicle manufacturer. In this thesis, we use the parameters corresponding to a 1994 Ford Fiesta (UK DOT, 1994). All vehicles in the simulation are of this model. This assumption can be easily relaxed. Microscopic simulators represent individual vehicles and thus, accounting for the specific technologies and performance of various fleet compositions is straightforward. The values of the vehicle type-specific parameters used are listed below:

C_1 0.333 mℓ/s;
C_2 0.537 mℓ/s;
C_3 0.42 mℓ/s;
C_4 0.26 mℓ-s^2/m^2;
C_5 0.223 mℓ/s;
C_6 0.00335 mℓ/m;
V^m 13.89 m/s.

Equation (2.3) can also be expressed as:

$$FC_j = FC_j^I + FC_j^D + FC_j^A + FC_j^C, \tag{2.4}$$

where FC_j^M ($M \in \{I$ (idling), D (deceleration), A (acceleration), C (cruising)$\}$ is the fuel consumed by a given vehicle j in mode M during a given simulation time-step. We now analyze each component of Equation (2.4) separately.

The fuel consumption attributed to idling, FC_j^I, for a given vehicle j during a given simulation time-step is defined as the idling fuel consumption rate multiplied by the time spent in idling mode. Thus,

$$FC_j^I = C_{1j} t_j^I. \tag{2.5}$$

Aimsun (v6.1) uses a constant value of idling fuel consumption rate C_{1j} as given in Ferreira (1982) (page 4). This value is based on data collected from instrumented vehicles in Leeds, UK for urban driving conditions.

The fuel consumption attributed to deceleration, FC_j^D, for a given vehicle j during a given simulation time-step is defined as the decelerating fuel consumption rate C_{2j} multiplied by the time spent in decelerating mode t_j^D. Thus,

$$FC_j^D = C_{2j} t_j^D. \tag{2.6}$$

We now detail the derivation of Equation (2.6) based on the work of Ferreira (1982) and for this derivation, we use the same notation as in Ferreira (1982). The fuel consumed by a vehicle, F_d, when it decelerates from an initial speed V_i to a final speed of zero is given by (Equation (3) on page 13 of Ferreira (1982)):

$$F_d = K_d(\frac{V_i}{R_d}), \tag{2.7}$$

where K_d is a regression constant and R_d is the deceleration rate or the rate of change of speed during deceleration. Thus,

$$R_d = \frac{\partial V_i}{\partial t}. \tag{2.8}$$

In Ferreira (1982) it is assumed that R_d is independent of time. On differentiating Equation (2.7) with respect to time we get the fuel consumption rate for deceleration, which is the same as C_{2j}. Thus,

$$\frac{\partial F_d}{\partial t} = C_{2j} = \frac{K_d}{R_d}(\frac{\partial V_i}{\partial t}). \tag{2.9}$$

Substituting the expression for R_d from Equation (2.8) in Equation (2.9) we get,

$$C_{2j} = K_d. \tag{2.10}$$

Thus, Aimsun (v6.1) assigns the value for the constant C_{2j} as equal to the regression constant K_d from Equation (3) of Ferreira (1982).

The fuel consumption attributed to acceleration, FC_j^A, for a given vehicle j during a given simulation time-step is defined as the accelerating fuel consumption rate

(which is a function of the vehicle's instantaneous speed v_j and instantaneous acceleration a_j) multiplied by the time spent in accelerating mode t_j^A. Thus,

$$FC_j^A = (C_{3j} + C_{4j} v_j a_j) t_j^A. \tag{2.11}$$

We now detail the derivation of Equation (2.11) based on the work of Ferreira (1982) and for this derivation, we use the same notation as in Ferreira (1982). The fuel consumed by a vehicle, F_a, when it accelerates from an initial speed of zero to a final speed V_f, is given by (Equation (5) on page 16 of Ferreira (1982)):

$$F_a = K_{1a}(\frac{V_f}{R_a}) + K_{2a}(V_f^2), \tag{2.12}$$

where K_{1a} and K_{2a} are regression constants and R_a is the acceleration rate or the rate of change of speed during acceleration. Thus,

$$R_a = \frac{\partial V_f}{\partial t}. \tag{2.13}$$

In Ferreira (1982), it is assumed that R_a is independent of time. On differentiating Equation (2.12) with respect to time we get the fuel consumption rate for acceleration. Thus,

$$\frac{\partial F_a}{\partial t} = \frac{K_{1a}}{R_a}(\frac{\partial V_f}{\partial t} + 2K_{2a} V_f (\frac{\partial V_f}{\partial t}). \tag{2.14}$$

Substituting the expression for R_a from Equation (2.13) in Equation (2.14) we get,

$$\frac{\partial F_a}{\partial t} = K_{1a} + 2K_{2a} V_f R_a. \tag{2.15}$$

During a simulation time-step, the vehicle speed V_f is denoted as the instantaneous vehicle speed v_j and the acceleration rate R_a is denoted as the instantaneous vehicle

acceleration a_j. Thus, Equation (2.15) can be re-written as,

$$\frac{\partial F_a}{\partial t} = K_{1a} + 2K_{2a} v_j a_j. \tag{2.16}$$

Substituting,

$$K_{1a} = C_{3j}, \qquad \text{and,} \qquad 2K_{2a} = C_{4j}, \tag{2.17}$$

in Equation (2.16), we get the fuel consumption rate for acceleration which is the same as that used by Aimsun (v6.1) and given in Equation (2.11).

The fuel consumption attributed to cruising, FC_j^C, for a given vehicle j during a given simulation time-step is defined as the cruising fuel consumption rate (which is a function of a vehicle's instantaneous speed v_j) multiplied by the time spent in cruising mode t_j^C. Thus,

$$FC_j^C = [C_{5j}(1 + \frac{v_j^3}{2(V_j^m)^3}) + C_{6j} v_j] t_j^C. \tag{2.18}$$

We now detail the derivation of Equation (2.18) based on the work of Akçelik (1983) and for this derivation, we use the same notation as in Akçelik (1983). According to the elemental model of fuel consumption (Equation (2) on page 51 of Akçelik (1983)) the fuel consumption per unit distance, f_c, for a vehicle cruising at a constant speed of v_c is given by:

$$f_c = b_1 + \frac{b_2}{v_c} + b_3 v_c^2, \tag{2.19}$$

where b_1, b_2 and b_3 are vehicle type-specific constants.

In order to get an approximation for the time derivative of fuel consumption in cruising mode (or fuel consumption rate), we multiply Equation (2.19) by the cruising speed v_c. This gives us,

$$\frac{\partial FC_j^C}{\partial t} \approx b_1 v_c + b_2 + b_3 v_c^3. \tag{2.20}$$

For a cruising speed of zero, the fuel consumption rate is equal to b_2. Thus b_2 is the idling fuel consumption rate provided by the vehicle manufacturer. The other coefficients b_1 and b_3 can in turn be derived from b_2 as shown below (Equation (2a) in Akçelik (1983)),

$$b_1 = f_0 - (\frac{1.5b_2}{v_0}) \qquad \text{and,} \qquad b_3 = \frac{b_2}{2v_0^3}, \tag{2.21}$$

where v_0 is the cruising speed at which fuel consumption is minimum and f_0 is the minimum fuel consumption rate while cruising (also provided by the vehicle manufacturer).

Substituting the expressions for b_1 and b_3 from Equation (2.21) in Equation (2.20) we get,

$$\frac{\partial FC_j^C}{\partial t} = b_2 + [f_0 - (\frac{1.5b_2}{v_0})]v_c + b_2(\frac{v_c^3}{2v_0^3}) \tag{2.22}$$

During a simulation time-step, the vehicle cruising speed v_c can be replaced by the instantaneous vehicle speed v_j. Also substituting,

$$b_2 = C_{5j}, \qquad v_0 = V_j^m, \qquad \text{and,} \qquad f_0 - (\frac{1.5b_2}{v_0}) = C_{6j} \tag{2.23}$$

in Equation (2.22), we get the fuel consumption rate for cruising which is the same as that used by Aimsun(v6.1) and given in Equation (2.18).

Macroscopic analytical model

The purpose of the analytical model is to provide an analytical, tractable (e.g., differentiable) macroscopic (i.e. aggregate) approximation of the microscopic fuel consumption model. We consider the entire simulation period (e.g., evening peak period). For this time period, the expected fuel consumption per vehicle on link ℓ, $E[FC_\ell]$, is approximated by using a simplified version of the Akçelik (1983) model. It is given

by:

$$E[FC_\ell] = \left(C_5(1 + \frac{E[V_\ell]^3}{2(V^m)^3}) + C_6 E[V_\ell] \right) E[T_\ell], \tag{2.24}$$

where C_5, C_6, V^m are vehicle type-specific parameters, $E[V_\ell]$ is the expected vehicle speed on link ℓ, and $E[T_\ell]$ is the expected vehicle travel time on link ℓ.

Equation (2.24) is derived by making the following two simplifications to the microscopic fuel consumption model. First, we account for a single operating mode, which is the cruising mode. That is, we assume that throughout the entire trip, the vehicle is in cruising mode. Secondly, we define the fuel consumption in cruising mode as a function of average vehicle speed (instead of instantaneous speed). If different vehicle types are to be used, similar macroscopic fuel consumption approximations can be derived for each vehicle type.

The approximations for $E[T_\ell]$ and $E[V_\ell]$ are derived as follows. The average link travel time $E[T_\ell]$ is derived by applying Little's law (Little, 1961) to the underlying queue:

$$E[T_\ell] = \frac{E[N_\ell]}{\lambda_\ell(1 - P(N_\ell = k_\ell))}, \tag{2.25}$$

where $E[N_\ell]$ is the expected number of vehicles in queue ℓ, λ_ℓ is the arrival rate to the queue, and $(1 - P(N_\ell = k_\ell))$ is the probability that the queue is not full (i.e. it can accept flow from upstream). For finite capacity queues the flow entering link ℓ is given by $\lambda_\ell(1 - P(N_\ell = k_\ell))$. For a description of how to apply Little's law to finite capacity queues, we refer the reader to Tijms (2003) (pages 52-53).

Both λ_ℓ and $P(N_\ell = k_\ell)$ are endogenous variables of the macroscopic traffic model. The expected number of vehicles, $E[N_\ell]$, is given by:

$$E[N_\ell] = \rho_\ell \left(\frac{1}{1 - \rho_\ell} - \frac{(k_\ell + 1)\rho_\ell^{k_\ell}}{1 - \rho_\ell^{k_\ell + 1}} \right), \tag{2.26}$$

where ρ_ℓ, is known as the traffic intensity, it is an endogenous variable of the macroscopic traffic model. The derivation of Equation (2.26) is detailed in Osorio (2010)

(pages 69-70).

The average speed is approximated by using the fundamental relationship that relates the average flow q to average speed v and density k: $q = kv$, which in this context is given by:

$$\lambda_\ell(1 - P(N_\ell = k_\ell)) = \frac{E[N_\ell]}{\mathsf{L}_\ell} E[V_\ell], \tag{2.27}$$

where L_ℓ denotes the length of link ℓ. In this equation the flow of a link is given as in Equation (2.25) by $\lambda_\ell(1 - P(N_\ell = k_\ell))$, and the average link density is approximated by $E[N_\ell]/\mathsf{L}_\ell$.

We then use $E[FC_\ell]$ of Equation (2.24) to approximate the expected total fuel consumption in the network by:

$$E[FC] = (\sum_{\ell \in \mathcal{L}} E[FC_\ell])\gamma, \tag{2.28}$$

where $\mathcal{L}$ is the set of all links in the network and γ is the expected number of trips during the considered simulation period (given, for instance, by the origin-destination matrix). This approximation may overestimate fuel consumption: by multiplying the expected fuel consumption per vehicle by the total demand, it is similar to assuming that all vehicles have traveled along all links. An alternate approximation such as $\sum_{\ell \in \mathcal{L}}(E[FC_\ell]\gamma_\ell)$ (where γ_ℓ is the expected demand for link ℓ) may be more accurate. To summarize, the analytical approximation of the expected total fuel consumption in the network is obtained by solving Equations (2.24)-(2.28).

2.3 Optimization problems

In this section, we formulate the three different traffic signal control problems that are addressed in this chapter. For a review of traffic signal control terminology and formulations, we refer the reader to Appendix A of Osorio (2010). In this thesis, we consider a fixed-time (also called time of day or pre-timed) control strategy. These are strategies that use historical traffic patterns to derive a fixed signal plan for a

given time period. The signal control problem is solved offline. The signal plans of multiple intersections are determined jointly. The decision variables are the green splits (i.e., green times) of phases of the different intersections. All other traditional control variables (e.g., cycle times, offsets, stage structure) are assumed fixed.

To formulate this problem we introduce the following notation:

b_i	available cycle ratio of intersection i;
$x(j)$	green split of phase j;
x_L	vector of minimal green splits;
$\mathscr{I}$	set of intersection indices;
$\mathscr{P}_I(i)$	set of phase indices of intersection i.

The problem is traditionally formulated as follows:

$$\min_x g(x;p) \equiv E[G(x;p)] \tag{2.29}$$

subject to

$$\sum_{j \in \mathscr{P}_I(i)} x(j) = b_i, \ \forall i \in \mathscr{I} \tag{2.30}$$

$$x \geq x_L, \tag{2.31}$$

where the decision vector x consists of the green splits for each phase. Constraints (2.30) ensure that for a given intersection the available cycle time is distributed among all phases. Green splits have lower bounds (Equation (2.31)), which are set to 4 seconds in this work (following the Swiss transportation norms VSS (1992)).

This chapter considers three different problems that vary according to their objective functions. The objective functions considered are:
1) expected travel time in the network (denoted g^T)
2) expected total fuel consumption in the network (denoted $g^{T,FC}$)
3) a linear combination of expected travel time in the network and expected total fuel

consumption in the network (denoted as $g^{T,FC}$) which is given by:

$$g^{T,FC} = (1 - w^{FC})g^T + (w^{FC})g^{FC}, \tag{2.32}$$

where w^{FC} is a weight parameter ($0 \leq w^{FC} \leq 1$). We use the weights as defined in Li et al. (2004), i.e., $w^FC = 3/7$.

Within the framework of each objective function, at each iteration of the SO algorithm, a trust region subproblem is solved. The formulation of this problem is given in Appendix B.

2.4 Empirical Analysis

2.4.1 Experimental setup

As described in Section 2.2.2, in this study we use a model of the city of Lausanne that represents evening peak period traffic (Dumont and Bert, 2006). We consider the first hour of the evening peak period (5-6pm). The network under consideration is located in the city center and is delimited by a circle in Figure 2-1, the detailed network is displayed in the left plot of the figure. This network contains 47 roads and 15 intersections of which 9 are signalized. The signalized intersections have a cycle time of either 90 or 100 seconds and a total of 51 variable phases. This is a complex constrained simulation-based optimization problem.

The queueing model of the network consists of 102 queues. The trust region subproblem (formulated in Appendix B) consists of 621 variables with their corresponding lower bound constraints, 408 nonlinear equality constraints, 171 linear equality constraints and one nonlinear inequality constraint. This is a high-dimensional simulation-based optimization problem.

We compare the performance of the following three optimization methods.

- The proposed approach, denoted Am.
- A traditional SO metamodel method, where the metamodel consists only of a

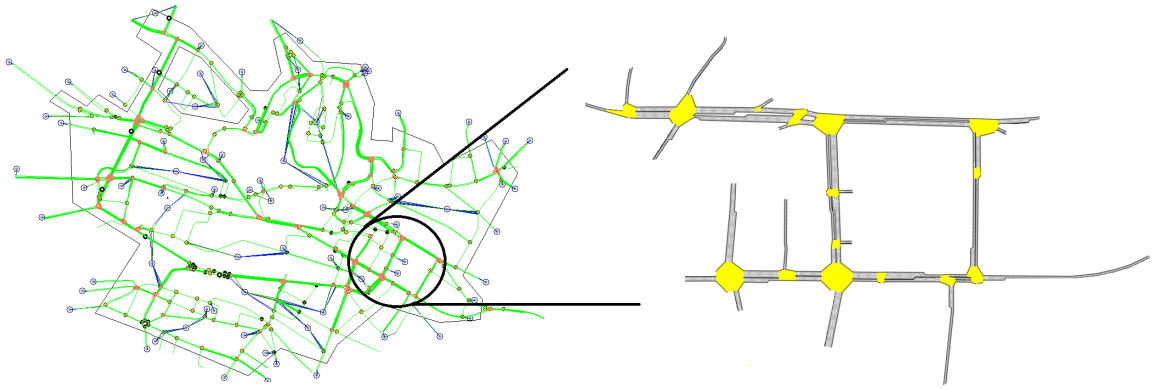

Figure 2-1: Lausanne city network model (left), network of interest (right).

quadratic polynomial with diagonal second derivative matrix (i.e., the meta-model consists of ϕ given in Equation (2.2)). This approach therefore uses simulation information but does not use information from the analytical traffic model (i.e., it does not have a physical component). This approach is denoted $A\phi$.

- A method that uses only the analytical traffic model, and does not use any simulated information (i.e., the objective function is given by g^A in Equation (2.2)). This method is denoted Ag^A.

We compare the performance of these three methods for three different objective functions g^T, g^{FC} and $g^{T,FC}$ as defined in Section 2.3.

We consider different types of initial points, namely, an existing fixed-time signal plan for Lausanne city (for details see Dumont and Bert (2006)), and randomly drawn feasible signal plans. The latter are uniformly drawn from the feasible region defined by Equations (2.30) and (2.31). We draw uniformly from this space using the code of Stafford (2006).

For methods Am and $A\phi$, we define the computational budget as a maximum of 150 simulation runs that can be carried. That is, the algorithm starts off with no simulated information, and once it has called the simulator 150 times it stops. The point considered as the current iterate (best point found so far) is taken as the proposed signal plan. This is a very tight computational budget, given the dimension

and complexity of the considered problems.

The derivation of a proposed signal plan involves calling the simulator. Given the stochastic nature of the simulation outputs, for a given initial point, the methods Am and $A\phi$ are run 5 times (allowing each time for a maximum of 150 runs). We then compare the performance of all 5 proposed signal plans.

We evaluate the performance of a proposed signal plan as follows. We embed the proposed signal plan within the Lausanne simulation model. We then run 50 simulation replications, which yield 50 observations of the performance measures of interest (travel time, fuel consumption, emissions). For a given performance measure, we plot the cumulative distribution function (cdf) of these 50 observations.

2.4.2 Results

We first compare the performance of the three methods for a combined objective function $g^{T,FC}$. Figure 2-2 considers a given initial point, and displays the performance of various signal plans in terms of total fuel consumption (left plot) and average travel time (right plot). Each plot displays 12 cdf curves: the 5 solid black (resp. dashed red) cdf's correspond to the cdf's of the signal plans proposed by Am (resp. $A\phi$). The green cdf corresponds to the signal plan proposed by Ag^A, and the blue is that of the initial signal plan. Each cdf curve consists of 50 observations which correspond to the 50 simulation replications. The optimization methods were initialized with a random (uniformly drawn) initial signal plan (blue cdf).

Figure 2-2(a) indicates that 3 of the signal plans derived by Am outperform, in terms of total fuel consumption, all other signal plans, and in particular all those derived by $A\phi$. The other 2 signal plans derived by Am have similar performance to the plans derived by $A\phi$. The signal plans derived by Am also have reduced variability compared to those of $A\phi$. All plans proposed by both Am and $A\phi$ have improved performance compared to the initial plan, and four out of five (for each method) have improved performance compared to the signal plan proposed by Ag^A. Figure 2-2(b) considers the same signal plans and displays their performance in terms of average travel time. Similar conclusions hold.

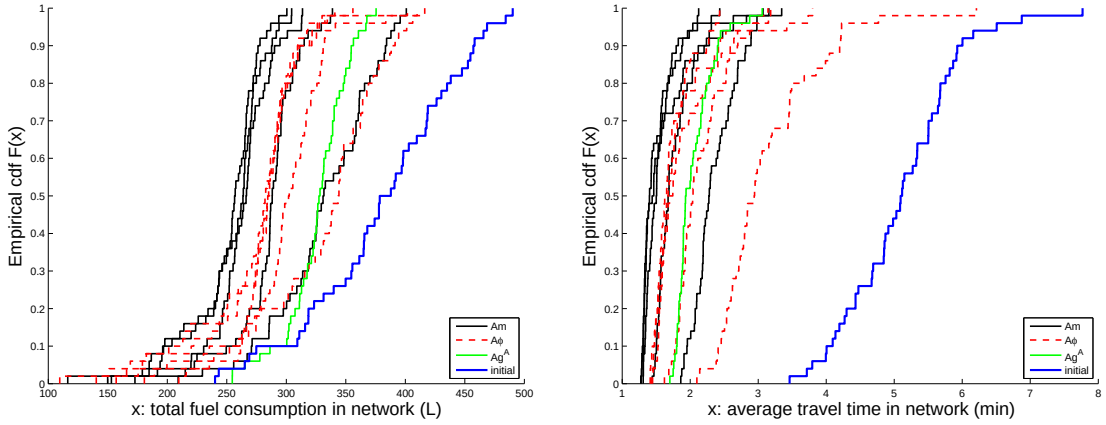

(a) (b)

Figure 2-2: Performance of the signal plans derived with the $g^{T,FC}$ objective function and a random initial signal plan.

Figure 2-3 considers a different random (uniformly drawn) initial signal plan. Figure 2-3(a) displays the cdf's of total fuel consumption. The four best signal plans are derived by Am, these plans also have the smallest variance in total fuel consumption. The fifth plan derived by Am has the worst performance. Similar conclusions hold, when evaluating the signal plans in terms of average travel time (Figure 2-3(b)).

Figure 2-4(a) considers an existing signal plan for the city of Lausanne as the initial plan. Four of the five plans derived by Am are among the best signal plans. The fifth has similar performance to the existing Lausanne plan. One of the signal plans derived by $A\phi$ has worse performance compared to the initial plan. The signal plan derived by Ag^A has similar performance to that of the initial signal plan. The same conclusions hold when evaluating the signal plans in terms of average travel time (Figure 2-4(b)).

In Figures 2-2, 2-3 and 2-4, 13 of the 15 plans derived by Am outperform the plans derived by Ag^A, in terms of both fuel consumption and travel time. This shows the added value of using both analytical and simulated information as opposed to only analytical information.

The information of Figures 2-2(a), 2-3(a) and 2-4(a) is summarized in Figure 2-5(a). The latter displays two cdf's one for all signal plans derived by Am (solid black) and one for all those derived by $A\phi$ (dashed red). Each cdf consists of all fuel

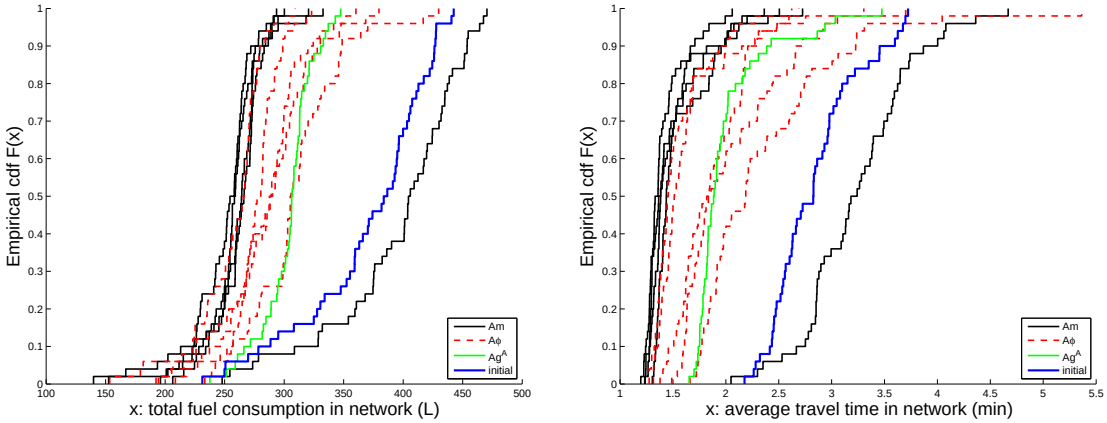

(a) (b)

Figure 2-3: Performance of the signal plans derived with the $g^{T,FC}$ objective function and a random initial signal plan.

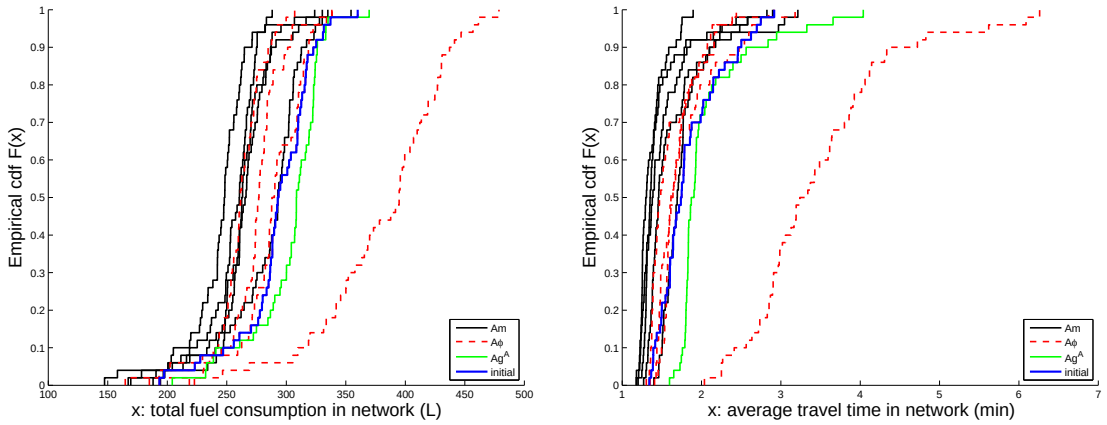

(a) (b)

Figure 2-4: Performance of the signals plan derived with the $g^{T,FC}$ objective function. The algorithms are initialized with an existing signal plan for Lausanne.

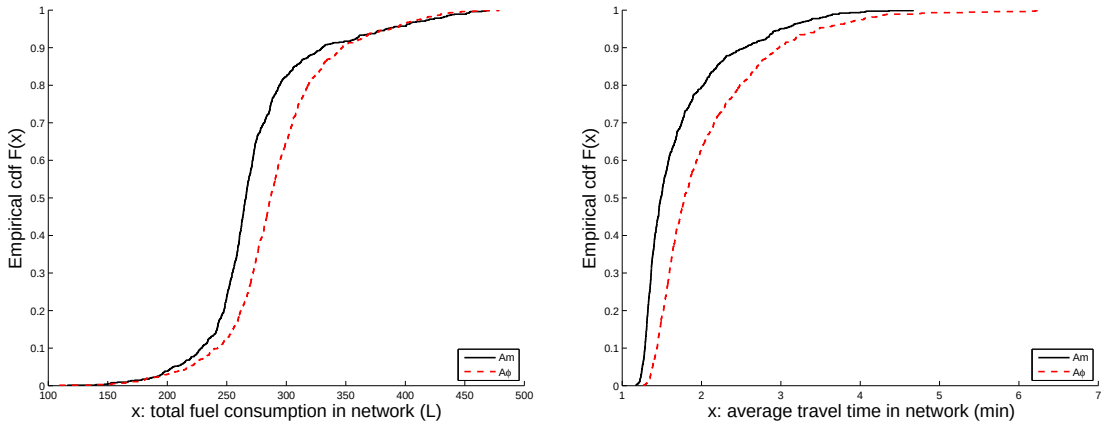

(a) (b)

Figure 2-5: Summary of the performance of the signal plans derived with the $g^{T,FC}$ objective function.

consumption observations displayed in the three previously mentioned figures (i.e., each cdf consists of $50 \times 5 \times 3 = 750$ total fuel consumption observations). Similarly, Figure 2-5(b) summarizes the information of Figures 2-2(b), 2-3(b) and 2-4(b). In both cases, the signal plans proposed by Am outperform those proposed by $A\phi$. These figures show that there is an added value of complementing the simulated information with analytical information.

Figure 2-6 considers the same initial point as Figure 2-2 and the objective function $g^{T,FC}$. Each plot displays the network of interest. Each link is colored according to the average (over 50 replications) fuel consumption per vehicle (in liters). The top plot considers the performance under the initial signal plan, whereas the bottom plot displays the performance of a signal plan derived by Am. This figure illustrates the fuel consumption reductions that can be achieved at the link level by the proposed signal plan.

Next, to understand the effect of different objective functions on the performance of the signal plans, Figures 2-7, 2-8, 2-9 and 2-10 consider a signal control problem with an objective function that accounts only for total fuel consumption (g^{FC}) in the network. This is a challenging problem, since the fuel consumption is a highly variable metric. Additionally, we are attempting to identify a signal plan with 51 variable phases (dimension of the decision vector) by calling the simulator at most

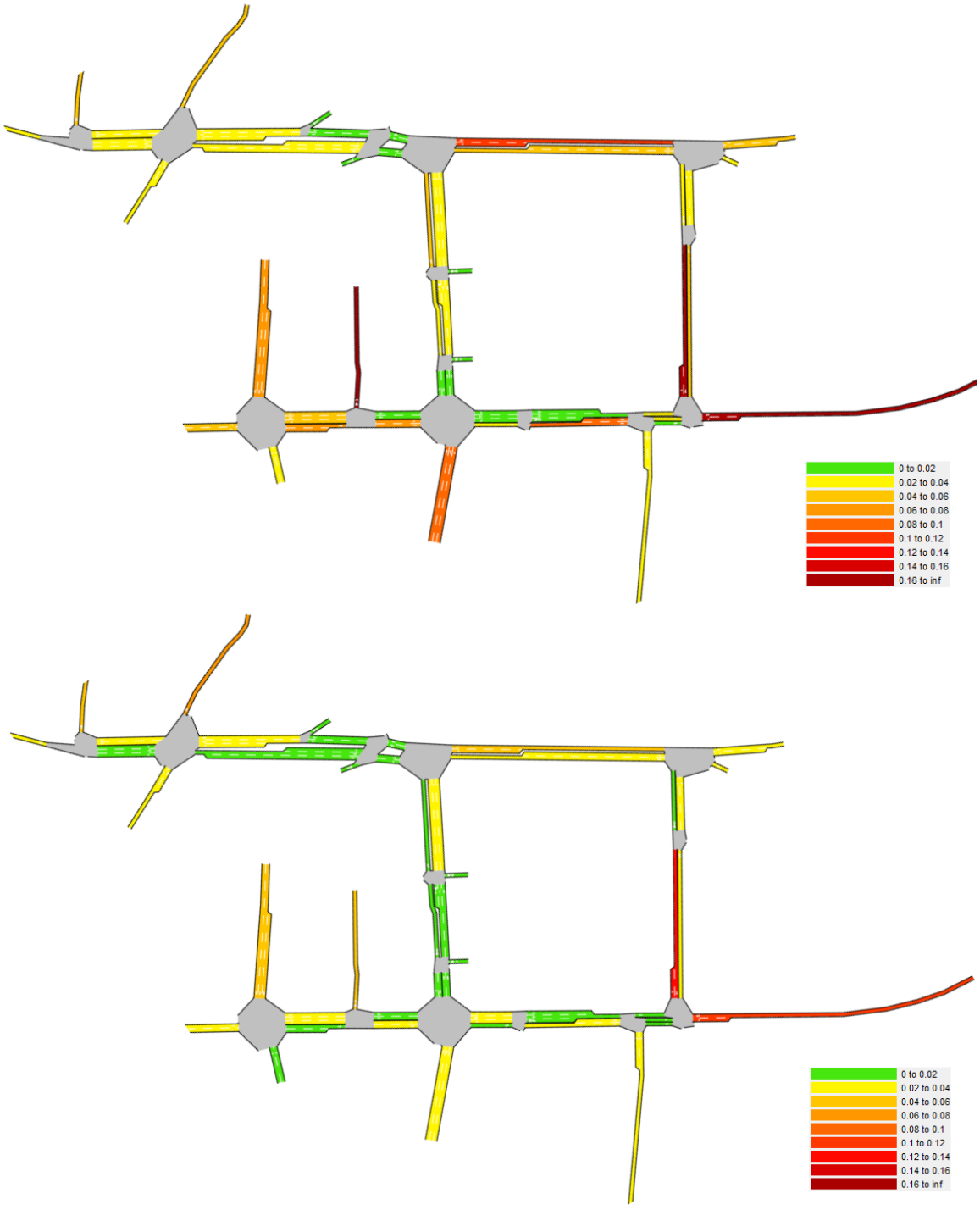

Figure 2-6: Average fuel consumption per vehicle per link (in liters).

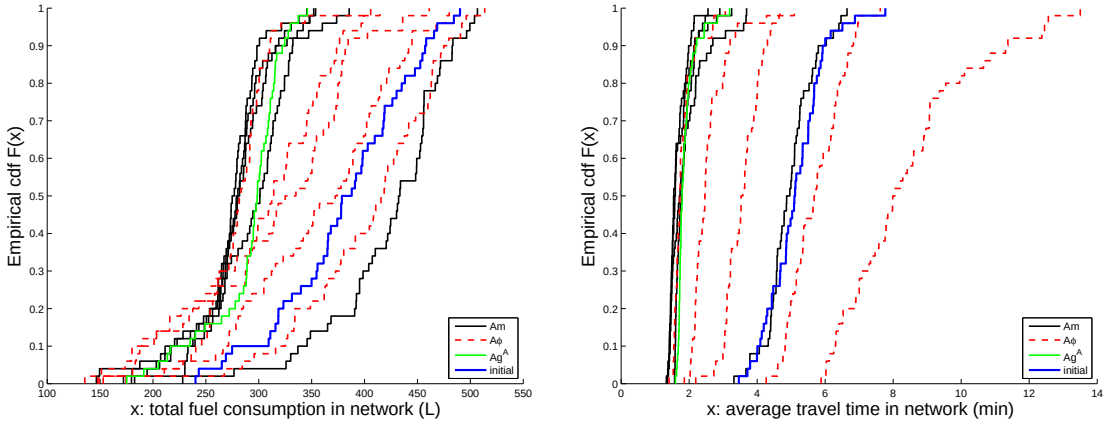

(a) (b)

Figure 2-7: Performance of the signal plans derived with the g^{FC} objective function and a random initial signal plan.

150 times.

In order to evaluate the performance of the signal plans, we proceed as before. That is we evaluate their performance both in terms of fuel consumption and of travel time. Figure 2-7 considers the same initial plan as Figure 2-2. Figure 2-7(a) indicates that of the top 4 signal plans with best performance, 3 are proposed by Am. Four of the plans proposed by Am outperform four of the plans proposed by $A\phi$. These four plans also lead to reduced variability. Both Am and $A\phi$ derived one signal plan with worse performance than the initial plan. When evaluating these plans in terms of their travel times (Figure 2-7(b)), four of the plans proposed by Am are among those with the best performance, whereas the fifth has performance similar to the initial plan.

Figure 2-8 considers the same initial plan as Figure 2-3. Figure 2-8(a) compares the total fuel consumption of the signal plans. Here the top 4 signal plans with best performance are proposed by Am. These plans also have reduced variability compared to those proposed by $A\phi$ and to the initial signal plan. Similar conclusions hold when evaluating these signal plans in terms of average travel time (Figure 2-8(b)).

Figure 2-9 considers the existing Lausanne signal as the initial plan (i.e. same initial plan as Figure 2-4). For both fuel consumption (Figure 2-9(a)) and travel time (Figure 2-9(b)) four out of the top 5 signal plans are proposed by Am. As before,

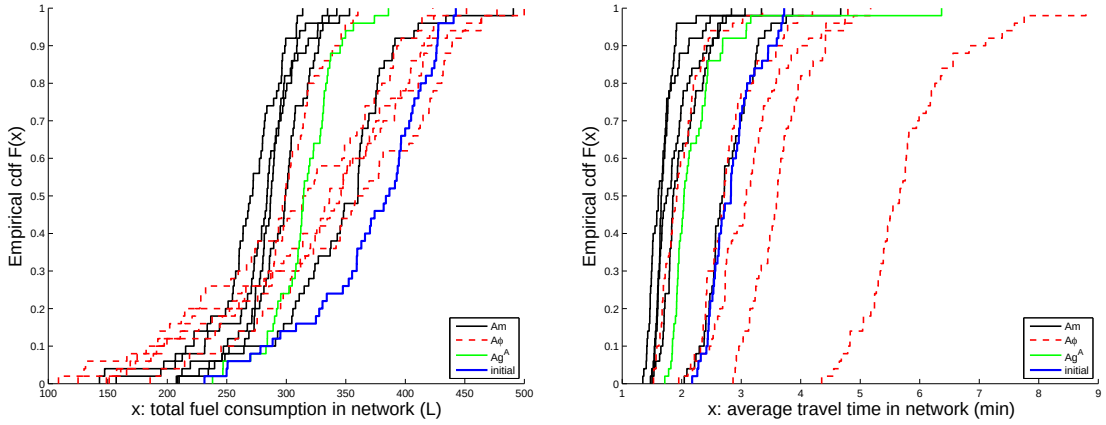

(a) (b)

Figure 2-8: Performance of the signal plans derived with the g^{FC} objective function and a random initial signal plan.

the plans proposed by Am lead to reduced variability compared to those proposed by $A\phi$.

Figure 2-10(a) summarizes the information of Figures 2-7(a), 2-8(a) and 2-9(a). It indicates that the signal plans proposed by Am outperform those proposed by $A\phi$ both in terms of total fuel consumption and average travel time.

Next, in Figures 2-11, 2-12, 2-13 and 2-14, we analyze the performance of the signal plans when the objective function excludes fuel consumption and considers only travel time (denoted as g^T). This objective has reduced variability since travel-time is not influenced to a significant degree by individual vehicle attributes, unlike fuel consumption. We proceed as before, evaluating the performance of each signal plan in terms of travel time and fuel consumption, and comparing the performance of the frameworks Am, $A\phi$ and Ag^A for a given initial plan.

Figure 2-11 considers the same initial point as Figures 2-2 and 2-7. Here, all five signal plans proposed by Am show similar improvements over the initial signal plan, both in terms of total fuel consumption and in terms of average travel time. The signal plan proposed by Ag^A also performs similarly to the Am plans. Of the five signal plans proposed by $A\phi$, three perform very similarly to Am while two do worse. Thus overall, we see that the variability in the performance of signal plans, both within a given framework and between different frameworks, is reduced.

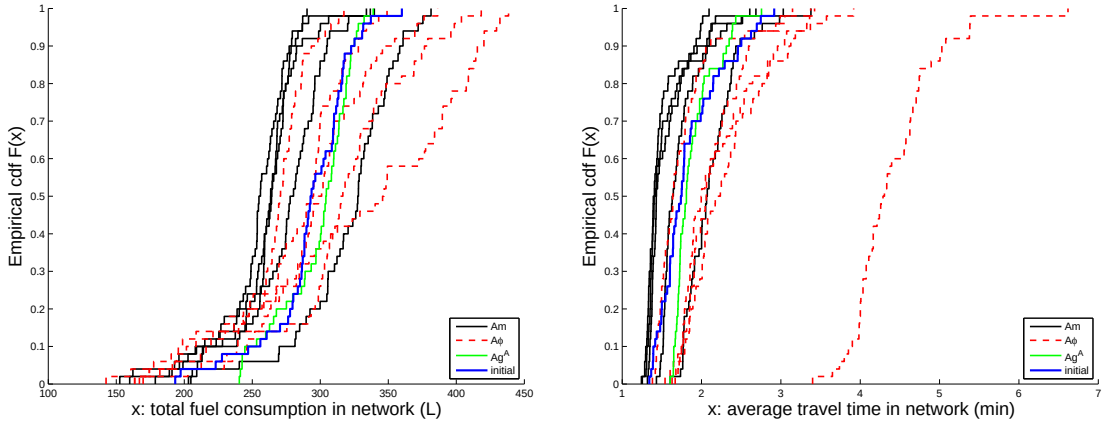

(a) (b)

Figure 2-9: Performance of the signal plans derived with the g^{FC} objective function. The algorithms are initialized with an existing signal plan for Lausanne

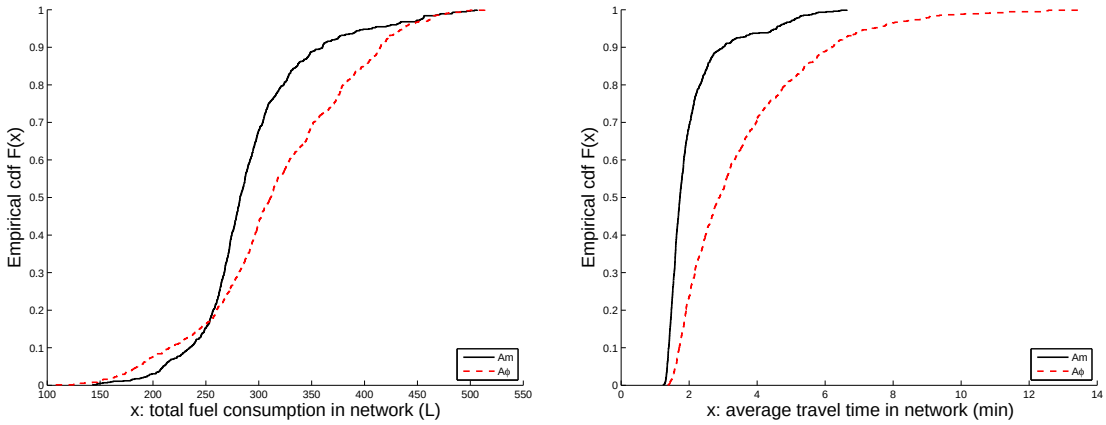

(a) (b)

Figure 2-10: Summary of the performance of the signal plans derived with the g^{FC} objective function.

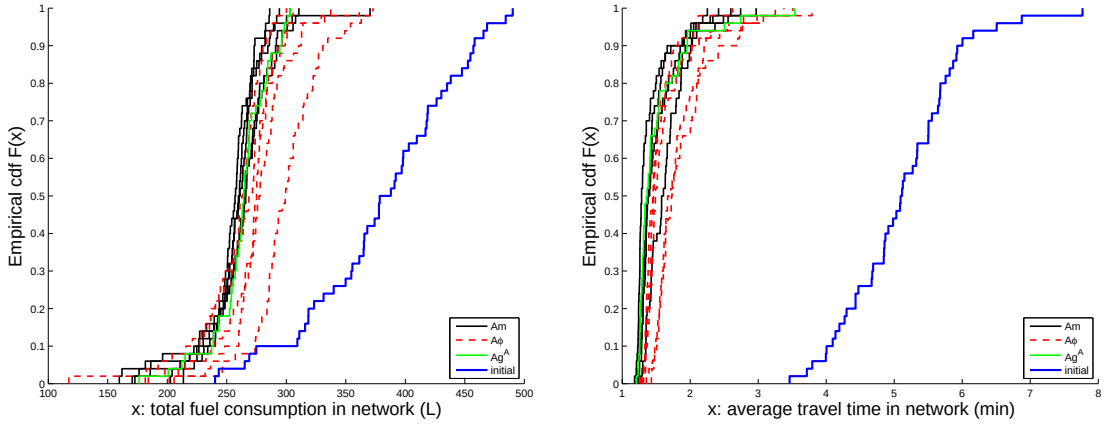

(a) (b)

Figure 2-11: Performance of the signal plans derived with the g^T objective function and a random initial signal plan.

Figure 2-12 considers the same initial point as Figures 2-3 and 2-8. In Figure 2-12(a), four of the five signal plans proposed by A_m perform similarly as the five plans derived by $A\phi$ and the single plan proposed by Ag^A. One of the plans proposed by Am does not do as well. In Figure 2-12(b), four of the signal plans proposed proposed by Am perform very well and similar to the plan proposed by Ag^A. The plans proposed by $A\phi$ comes next in terms of performance. The fifth plan proposed by Am does not do as well.

Figure 2-13 considers the existing signal plan of Lausanne as the initial plan (i.e. the same initial plans as Figures 2-4 and 2-9). The five plans proposed by Am perform similarly, both in terms of total fuel consumption and in terms of average travel time, to four of the plans proposed by $A\phi$ and the single plan proposed by Ag^A. One of the plans proposed by $A\phi$ performs worse than the initial signal plan.

Figure 2-14 summarizes the information in Figures 2-12, 2-11 and 2-12. The signal plans proposed by Am outperform those proposed by $A\phi$. However, the improvement is lower than that seen in Figures 2-5 and 2-10.

2.4.3 Case study conclusions

Figures 2-2 to 2-14 show that there is an added value of combining simulated and analytical information. Since fuel consumption observations depend strongly on in-

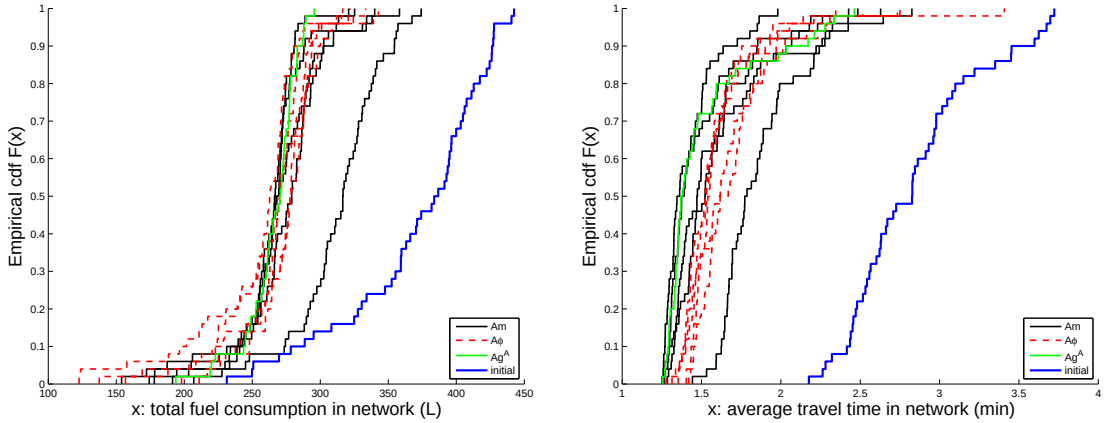

(a) (b)

Figure 2-12: Performance of the signal plans derived with the g^T objective function and a random initial signal plan.

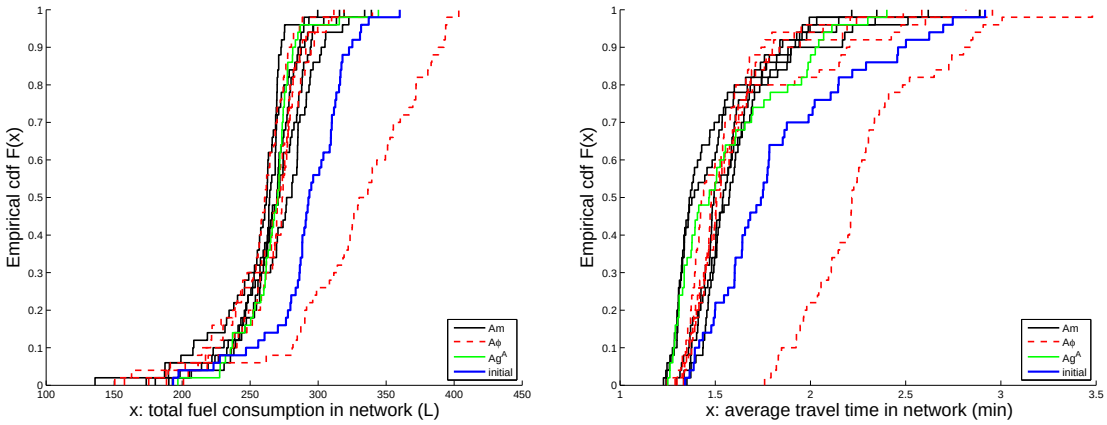

(a) (b)

Figure 2-13: Performance of the signal plans derived with the g^T objective function. The algorithms are initialized with an existing signal plan for Lausanne

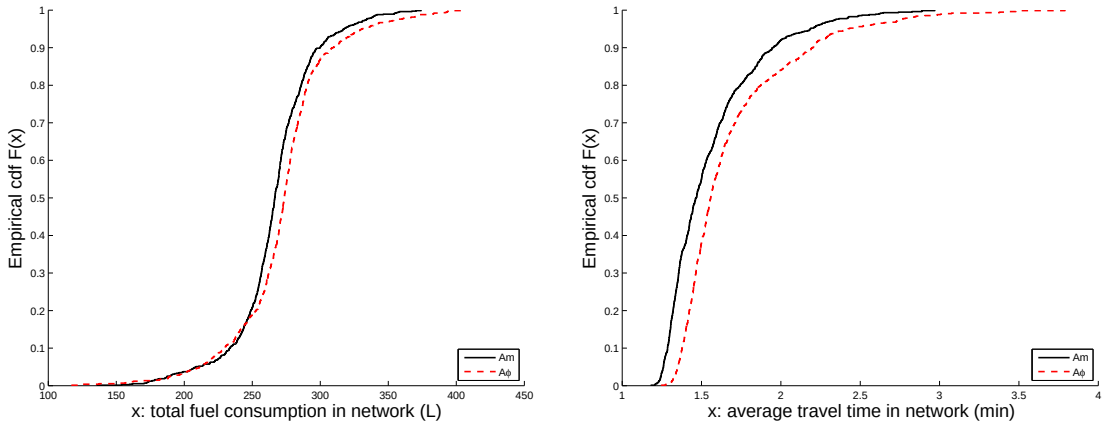

(a) (b)

Figure 2-14: Summary of the performance of the signal plans derived with the g^T objective function.

dividual vehicle attributes and complex local traffic dynamics, they have high variability. Thus, an algorithm which uses only simulated information is typically at a disadvantage compared to one that combines suitable analytical and simulated information. In Chapter 3 we formulate a signal control problem that addresses a more complex objective involving multiple noisy metrics. Once again, the performance of the proposed framework Am is compared to that of the other frameworks $A\phi$ and Ag^A, and the empirical results are presented for a traffic network in Lausanne.

Chapter 3

Signal control for emissions mitigation

3.1 Literature review

Just as fuel consumption models, emissions models can be either macroscopic or microscopic in their modeling of vehicle emissions (for reviews see Cappiello (2002), Rakha et al. (2003), Williams and Yu (2001)). Macroscopic emissions models are usually based on laboratory drive cycle tests conducted at a given average speed/acceleration (CARB, 2008, EPA, 1994). Once the emissions rates are established for a given average speed, the emissions at other average speeds are estimated by multiplying by speed correction factors (SCFs). SCFs are based on inputs of vehicle-specific characteristics such as age and operating conditions, and use a single variable namely average speed to determine emissions. Thus, they do not account for time-variations in speed and acceleration which may significantly impact emissions and lead to erroneous conclusions (Rakha et al., 2000). However since they do not require second-by-second speed or acceleration information, they offer relative ease of computation when applied to emissions over large areas (Bartin et al., 2007, Bai et al., 2007). Microscopic emissions models on the other hand, take into account the detailed interaction between drivers and the instantaneous speed and acceleration of each vehicle in the network. They are considered to be more accurate but due to the complexity of computations

involved, they have primarily been applied to segments of a corridor (Stathopoulos and Noland, 2003) or small networks within a city (Stevanovic et al., 2009).

Microscopic emissions models are primarily of two kinds: load-based (EPA, 2010, Scora and Barth, 2006) and regression-based (Rakha et al., 2004, Smit et al., 2007). Both kinds of models require instantaneous speed and acceleration data as inputs along with parameters such as vehicle manufacturer, vehicle age, road-grade etc. Regression models require additional inputs of on-road emissions information from instrumented vehicles. Load-based microscopic emissions models use the input data to identify different speed and acceleration events in a vehicle's path from origin to destination. Next, equations which quantify the impact of each speed/acceleration event on the engine load are used to estimate emissions. Thus, the emissions estimates from load-based models have a physical interpretation but are more complex to construct since it requires an understanding of the mechanical phenomena in a vehicle's engine. Regression-based microscopic emissions models on the other hand, fit a polynomial to the emissions data collected from instrumented vehicles. Thus, they are easier to construct but the regression constants used to fit the model do not necessarily have a physical interpretation. In this section, we review recent work that has coupled traffic simulators with emissions models to address urban transportation problems.

Li et al. (2004) use an analytical model that describes the movements of vehicles arriving and leaving an intersection in Nanjing City, China, based on the traffic signal settings for the intersection. The cycle length for the intersection is treated as a variable. The authors derive an optimal cycle length for the intersection by plotting a graph showing the effect of different cycle lengths on a weighted objective function containing average vehicle delay, total fuel consumption and total emissions at the intersection. The fuel consumption and emissions at the intersection are estimated using analytical expressions derived from prior studies (Xiang, 2000, Li, 1999). The weights for the three terms in the objective function are assigned as 4:3:3 respectively but the authors do not elaborate on how these weights were derived. Each term in the objective function is normalized with respect to the initial signal settings for

the intersection. The pollutants considered in this study are carbon monoxide(CO), hydrocarbons (HC) and nitrogen oxides (NO_x).

Williams and Yu (2001) observe the effects on travel time and emissions in a small hypothetical network when different traffic assignment objectives are used. They also observe the effects of changing the cycle length of the only signalized intersection in the network and the impact of signalizing an additional intersection. They use the macroscopic traffic model DYNAMIC (Yu, 1994) which has an inbuilt macroscopic emissions model. The movement of vehicles through the network is influenced by the assignment objectives and the number as well as the settings of traffic signals in the network, which in turn influences travel time and emissions. Here, the authors merely observe the changes in the performance metrics for before and after scenarios in each case.

Bai et al. (2007) combine the mesoscopic dynamic traffic assignment model DYNASMART-P (Mahmassani et al., 2004) with the macroscopic emissions model EMFAC (CARB, 2008) to study the effect of changes in regional demand on emissions. The authors investigate and compare two approaches to modeling regional emissions in the Sacramento and Kern counties of California, USA, namely the use of trip-average speeds and the use of link-average speeds. They find that the emissions calculated from the trip-based approach are more sensitive to changes in regional demand while those estimated using the link-based approach are sensitive to changes in specific roadway facilities (e.g., the introduction of a new highway lane or congestion on specific links).

Bartin et al. (2007) analyze the emissions impacts of introducing Electronic Toll Collection (ETC) systems on the New Jersey Turnpike, USA using a large-scale simulation network model implemented with the microscopic traffic simulator PARAMICS (Quadstone, 2009) in combination with the macroscopic emissions model MOBILE6.2 (EPA, 2003). The authors find that while emissions on the tollbooth links are reduced as a result of the ETC, the throughput of the Turnpike increases and the net system-wide effect is an increase in emissions. Interfacing between the microscopic traffic model and the macroscopic emissions model is achieved by computing the average

speed of each vehicle during each time-step (as defined in the traffic simulator) and providing this as input to the emissions model.

Xie et al. (2011) study the effect on pollutant emissions of carbon monoxide (CO), nitrogen oxides (NO_x), sulphur oxides (SO_x) and carbondioxide (CO_2) when a certain percentage of the car fleet is electric or uses biofuel. The effect on emissions when public transit buses switch to Compressed Natural Gas as fuel, is also studied. The case-study considered is a segment of a freeway in Greenville, South Carolina, USA which is modeled in the microscopic traffic simulator PARAMICS (Quadstone, 2009). The traffic model is coupled with the emissions model MOVES (EPA, 2010) which has the capability of estimating microscopic emissions using the load-based approach. However, in the study MOVES is used in a macroscopic context by providing as inputs to it only the link-level traffic counts and average speeds. Since the network modeled is not large, the decision to use MOVES as a macroscopic emissions model does not seem justified given the availability of detailed speed and acceleration information from PARAMICS.

Liu and Tate (2000) study the impacts on carbon monoxide (CO), hydrocarbon (HC) and nitrogen oxide (NO_x) emissions when vehicles equipped with Intelligent Speed Adaptation (ISA) systems are deployed on a road network in Leeds, UK. ISA-equipped vehicles have a speed control system that prevents them from exceeding the speed limit (on links which have specified limits). A fixed percentage of the vehicle fleet is assumed to have ISA and the interaction of these vehicles with other vehicles in the network is modeled using the microscopic traffic simulator DRACULA (Liu, 2005). The outputs of each simulation time-step namely, the time spent cruising along with the cruising speed, the time spent accelerating,time spent decelerating and time in idling mode, are supplied to the macroscopic emissions model QUARTET (QUARTET, 1992) which specifies an emissions rate for each combination of pollutant and operating mode. The authors analyze the effect of ISA systems on emissions for different levels of penetration of these systems in the vehicle fleet, for different congestion levels, for different roadway types and for different pre-determined speed-limit settings.

Cappiello (2002) develops a microscopic emissions model called EMIT which has the capability to estimate emissions of carbondioxide (CO_2), carbon monoxide (CO), hydrocarbons (HC) and nitrogen oxides (NO_x). EMIT is defined using the load-based approach i.e. it uses equations to specify engine-load based on instantaneous speed and acceleration. However, the constants used in these equations are calibrated using regression-techniques drawing from an existing database of vehicle emissions from on-road instrumented vehicles. EMIT is combined with a mesoscopic traffic simulator developed by Bottom (2000). The traffic management problem addressed in this study has been described in Section 2.1.

Zegeye et al. (2010) integrate the macroscopic traffic model METANET (Messmer and Papageorgiou, 1990) with the microscopic fuel consumption/emissions model VT-Micro (Rakha et al., 2004). The traffic control problem addressed in this study has been described in Section 2.1.

Lin et al. (2011) combine the mesoscopic traffic simulator DynusT (Chiu et al., 2011) with the microscopic emissions model MOVES (EPA, 2010) in order to evaluate the impact of congestion management schemes in Sacramento, California, USA on emissions of carbondioxide (CO_2). While DynusT does not directly provide instantaneous acceleration being a mesoscopic model, it is estimated as the difference in instantaneous speed between two time-steps and then supplied as input to MOVES.

Rakha et al. (2000) apply the microscopic fuel/emissions model VT-Micro in combination with the microscopic traffic simulator INTEGRATION (Van Aerde, 1999) to evaluate signal control strategies as described in Section 2.1.

Lee et al. (2009) use the microscopic traffic simulator TransModeler (Caliper, 2008) in combination with the microscopic emissions model CMEM (Scora and Barth, 2006) and the macroscopic emissions model EMFAC (CARB, 2008) in order to estimate the impact of heavy-duty truck movements along a highway connecting to a container port facility in Alameda, California, USA, on emissions of carbon monoxide (CO), carbondioxide (CO_2), hydrocarbons (HC), nitrogen oxides (NO_x) and particulate matter (PM). While CMEM has the capability of modeling the first four pollutants it does not provide estimates of particulate matter which constitutes the biggest health risk

among the five. So the authors use EMFAC for this purpose. The emissions impacts of several strategies such as cleaner fuel for trucks, alternate modes such as rail connecting to the container facility, lane restrictions on the highway etc.

Madireddy et al. (2011) integrate the microscopic traffic simulator PARAMICS (Quadstone, 2009) with the microscopic emissions model VERSIT+ (Smit et al., 2007) to evaluate traffic management schemes in Antwerp, Belgium. The effect of speed limit reduction in certain residential areas on emissions of carbon dioxide (CO_2) and nitrogen oxides (NO_x) is studied. The speed limits on the residential roads included in the network are lowered to a pre-determined value and the resulting emissions are compared to the original scenario.

Panis et al. (2006) develop a regression-based microscopic emissions model in their study, fitted to emissions data collected from on-road instrumented vehicles in Leeds, UK. The emissions model is coupled with the microscopic traffic simulator DRACULA (Liu, 2005) to study the effect on emissions of carbondioxide (CO_2), nitrogen oxides (NO_x), volatile organic compounds (VOC) and particulate matter (PM) when a given percentage of the fleet in Ghent, Belgium is fitted with ISA systems. While ISA systems result in a lowered average speed for the network, the authors find that these systems have almost no noticeable effect on emissions. The authors state a possible reason for this to be that ISA-equipped vehicles have lower cruising speeds and lower speed variations. The authors believe that the two effects of having lower speeds (leading to higher emissions in this case) but with less speed variation (leading to lowered emissions again specific to this case) may be the reason for this observation.

To summarize, traffic models coupled with emissions models have been used at the macroscopic, mesoscopic and microscopic scales. Microscopic simulators coupled with microscopic emissions models are the most accurate since they account for detailed vehicle interaction which is known to influence emissions to a significant degree. However, most of the prior work using a combination of microscopic traffic simulators with microscopic emissions models have been what-if analyses i.e. the emissions model is used to evaluate pre-determined traffic management strategies as opposed to being used to identify viable strategies. To the best of our knowledge, the only work

that has integrated microscopic traffic and emissions models to perform optimization is that of Stevanovic et al. (2009). A review of their study can be found in Chapter 2.

In the next section, a simulation-based optimization (SO) technique is proposed that uses integrated traffic and emissions models to address a signal control problem for a city network in Lausanne. We see that the proposed SO framework is able to identify signal plans with improved performance on many different metrics and it is able to do so within a tight computational budget. This is especially challenging given the high degree of variability in emissions estimates from one simulation run to the next. The proposed method can be used to inform traffic control decisions at the network-level while using disaggregate and noisy vehicle-specific information.

3.2 Methodology

3.2.1 Simulation-based optimization framework

The simulation-based optimization framework used in this chapter is identical to the one presented in Section 2.2.1 with the exception that the performance measure G used in Equation (2.1) is now a combination of travel time and various pollutant emissions. This performance measure is also expected to show a high degree of variability from one simulation run to the next since it is dependent on vehicle-specific attributes which include but are not limited to vehicle type, engine technology, instantaneous speed and acceleration. Once again, we address the challenge of identifying, within a limited number of simulation runs, signal plans with improved performance using a high-variance performance measure.

3.2.2 Traffic models

We use a microscopic simulation model of the Swiss city of Lausanne (Dumont and Bert, 2006) and a macroscopic analytical queueing network model derived in Osorio and Bierlaire (2009b). For a brief description of these models please refer Section 2.2.2.

3.2.3 Emissions models

Microscopic emissions model

We use the microscopic emissions model embedded in Aimsun (v6.1), which is based on the model of Panis et al. (2006). This model gives the instantaneous emissions rate of four pollutants namely carbon dioxide (CO_2), nitrogen oxides (NO_x), volatile organic compounds (VOC) and particulate matter (PM), based on a vehicle's instantaneous speed and acceleration. We introduce the following notation for a given vehicle j:

k	Pollutant type, $k \in \{CO_2, NO_x, VOC, PM\}$;
$v_j(t)$	Instantaneous speed (in m/s);
$a_j(t)$	Instantaneous acceleration (in m/s^2);
$ER_j^k(t)$	Instantaneous emissions rate of pollutant k (in g/s);
E_{0j}^k	Minimum emissions rate of pollutant k (in g/s);
$C_{1j}^k, C_{2j}^k, C_{3j}^k, C_{4j}^k, C_{5j}^k, C_{6j}^k$	Emissions rate coefficients for pollutant k.

The emissions rate for vehicle j at a given time-instant t is given by (Equation (4) in Panis et al. (2006)):

$$ER_j^k(t) = max\{E_{0j}^k, C_{1j}^k + C_{2j}^k v_j(t) + C_{3j}^k v_j(t)^2 + C_{4j}^k a_j(t) + C_{5j}^k a_j(t)^2 + C_{6j}^k v_j(t) a_j(t)\}. \tag{3.1}$$

In Panis et al. (2006), the minimum emissions rate E_{0j}^k is fixed at zero for all pollutant types and vehicle types. The coefficients C_{1j}^k, C_{2j}^k, C_{3j}^k, C_{4j}^k, C_{5j}^k, C_{6j}^k are specified for each pollutant type and vehicle type based on a regression model fitted to emissions observations from on-road instrumented vehicles (Panis et al., 2006). However, for the purpose of this study only a single vehicle type i.e. petrol car, is considered. For a given pollutant type and vehicle type, the coefficients C_{1j}^k to C_{6j}^k may be different for acceleration and deceleration. Table 2 on page 276 of Panis et. al (2006) specifies different coefficients for the pollutants VOC and NO_x based

on whether $a_j(t)$ is positive or negative. The table gives the same coefficients for acceleration and deceleration for the pollutants CO_2 and PM. This distinction is made because the regression curves of the pollutants NO_x and VOC show differences between when they are fitted to acceleration data-points and when they are fitted to deceleration data-points while this is not the case for the pollutants CO_2 and PM. The reader is referred to Panis et. al (2006) for further details.

The values of the vehicle type-specific parameters used are listed below:

Common for acceleration and deceleration modes,

C_1^{CO2}	5.53 x 10^{-1} g/s;
C_2^{CO2}	1.61 x 10^{-1} g/m;
C_3^{CO2}	-2.89 x 10^{-3} g-s/m^2;
C_4^{CO2}	2.66 x 10^{-1} g-s/m;
C_5^{CO2}	5.11 x 10^{-1} g-s^3/m^2;
C_6^{CO2}	1.83 x 10^{-1} g-s^2/m^2;
C_1^{PM}	0;
C_2^{PM}	1.57 x 10^{-5} g/m;
C_3^{PM}	-9.21 x 10^{-7} g-s/m^2;
C_4^{PM}	0;
C_5^{PM}	3.75 x 10^{-5} g-s^3/m^2;
C_6^{PM}	1.89 x 10^{-5} g-s^2/m^2;

For acceleration mode,

C_1^{NOx}	6.19 x 10^{-4} g/s;
C_2^{NOx}	8 x 10^{-5} g/m;
C_3^{NOx}	-4.03 x 10^{-6} g-s/m^2;
C_4^{NOx}	-4.13 x 10^{-4} g-s/m;
C_5^{NOx}	3.80 x 10^{-4} g-s^3/m^2;
C_6^{NOx}	1.77 x 10^{-4} g-s^2/m^2;

C_1^{VOC}	4.47 x 10^{-3} g/s;
C_2^{VOC}	7.32 x 10^{-7} g/m;
C_3^{VOC}	-2.87 x 10^{-8} g-s/m^2;
C_4^{VOC}	-3.41 x 10^{-6} g-s/m;
C_5^{VOC}	4.94 x 10^{-6} g-s^3/m^2;
C_6^{VOC}	1.66 x 10^{-6} g-s^2/m^2;
For deceleration mode,	
C_1^{NOx}	2.17 x 10^{-4} g/s;
C_2^{NOx}	0;
C_3^{NOx}	0;
C_4^{NOx}	0;
C_5^{NOx}	0;
C_6^{NOx}	0;
C_1^{VOC}	2.63 x 10^{-3} g/s;
C_2^{VOC}	0;
C_3^{VOC}	0;
C_4^{VOC}	0;
C_5^{VOC}	0;
C_6^{VOC}	0.

Macroscopic analytical model

The purpose of the analytical emissions model is to provide a tractable (e.g., differentiable) macroscopic (i.e. aggregate) approximation of the microscopic emissions model. For vehicles on link ℓ, the expected emissions rate, ER_ℓ^k (in g/s), of pollutant type k (where $k \in \{CO_2, NO_x, VOC, PM\}$) is approximated by using a simplified version of the Panis et al. (2006) model as given by:

$$E[ER_\ell^k] = max\{E_0^k, C_1^k + C_2^k E[V_\ell] + C_3^k E[V_\ell]^2\} \tag{3.2}$$

where E_0, C_1, C_2 and C_3 are vehicle type-specific parameters, and $E[V_\ell]$ is the expected vehicle speed on link ℓ.

Equation (3.2) is derived by making the following two simplifications to the microscopic emissions model. First, we assume that throughout its trip in the considered network, a vehicle is in cruising mode. Thus, we substitute $a_j(t) = 0$ in Equation (3.1). Second, we assume that the emissions rate over a link ℓ for a vehicle in cruising mode is a function of average vehicle speed over that link (instead of instantaneous speed) and substitute $v_j(t)$ with $E[V_\ell]$ in Equation (3.1). If different vehicle types are to be used, similar macroscopic emissions approximations can be derived for each vehicle type.

The expected total emissions (in g) of pollutant k on link ℓ during the simulation is given by,

$$E[E_\ell^k] = E[ER_\ell^k]E[T_\ell]\lambda_\ell \Delta T \tag{3.3}$$

where $E[T_\ell]$ is the expected travel time on link ℓ, λ_ℓ is the arrival rate to the queue ℓ and ΔT is the total simulation time.

The analytical approximations to expected speed $E[V_\ell]$ and expected travel time $E[T_\ell]$ are detailed in Section 2.2.3.

The expected total emissions (in g) of pollutant k in the network during the simulation is given by,

$$E[E^k] = \sum_{\ell \in \mathcal{L}} E[E_\ell^k] \tag{3.4}$$

where $\mathcal{L}$ is the set of all links in the network.

3.3 Optimization problem

The general formulation of the traffic signal problem addressed in this section is given by Equations (2.29), (2.30) and (2.31) as described in Chapter 2. Here, we consider an objective function which is a linear combination of expected travel time g^T and

the expected total emissions of four pollutants in the network namely carbon dioxide, nitrogen oxides, volatile organic compounds and particulate matter, denoted as g^{CO2}, g^{NOx}, g^{VOC} and g^{PM} respectively, and given by:

$$g^{T,EM} = (\frac{w^T}{n^T})g^T + (\frac{w^{CO2}}{n^{CO2}})g^{CO2} + (\frac{w^{NOx}}{n^{NOx}})g^{NOx} + (\frac{w^{VOC}}{n^{VOC}})g^{VOC} + (\frac{w^{PM}}{n^{PM}})g^{PM} \quad (3.5)$$

where w^T, w^{CO2}, w^{NOx}, w^{VOC} and w^{PM} are economic weighting parameters for travel time and the pollutants CO_2, NO_x, VOC and PM respectively. While w^T denotes the value of time, the weights for each of the pollutants are based on their externality costs to human health and other large-scale effects such as global warming. The values of the weighting parameters are derived from Table 2 and Table 9 of Mayeres et al. (1996), and listed below:

w^T	2.14 x 10^{-3} EURO/s;
w^{CO2}	7.72 x 10^{-3} EURO/g;
w^{NOx}	13.8 x 10^{-3} EURO/g;
w^{VOC}	2.95 x 10^{-3} EURO/g;
w^{PM}	83.19 x 10^{-3} EURO/g;
n^T	109.32 s;
n^{CO2}	5.19 x 10^5 g;
n^{NOx}	818.09 g;
n^{VOC}	1.60 x 10^3 g;
n^{PM}	106.76 g.

n^T, n^{CO2}, n^{NOx}, n^{VOC} and n^{PM} are normalization constants for travel time, CO_2, NO_x, VOC and PM respectively, derived from the value of the respective performance measure for the existing signal configuration of the network.

Implementation Notes

The analytical approximation of the expected emissions rate g^k from Equation (3.5) where $k \in \{CO_2, NO_x, VOC, PM\}$, is a non-differentiable function given by Equa-

tion (3.2). This equation ensures that the emissions rate of a pollutant k on a link ℓ is always non-negative since the minimum emissions rate E_0^k is set to zero for all pollutants and vehicle types in Table 2 of Panis et al. (2006). However, the optimization problem we solve requires that the analytical approximation of the objective function $g^{T,EM}$ be differentiable at every point. During implementation, we make the following two changes in the macroscopic emissions model to ensure differentiability. First we define two new variables for each link (i.e. queue) ℓ, given by $y_{1\ell}$ and $y_{2\ell}$, which are related to the analytical approximation of the expected emissions rates on link ℓ ($\mathrm{E}[e_\ell^k]$) in the following way:

$$y_{1\ell} - y_{2\ell} = \sum_k \frac{w^k}{n^k}(C_1^k + C_2^k E[V_\ell] + C_3^k E[V_\ell]^2) \tag{3.6}$$

Second, we impose lower bounds (equal to zero) for $y_{1\ell}$ and $y_{2\ell}$. Equation (3.6) ensures that if the total emissions rate for a given link is positive, then it is equal to $y_{1\ell}$, and $y_{2\ell}$ equals zero. If the total emissions rate for the link is negative, then it is equal to the opposite of $y_{2\ell}$, and $y_{1\ell}$ equals zero. This implementation does not ensure that the emissions rate of each pollutant type k (where $k \in \{\mathrm{CO}_2, \mathrm{NO}_x, \mathrm{VOC}, \mathrm{PM}\}$) on link ℓ is non-negative. However, the total emissions rate on link ℓ is always non-negative.

Since only non-negative emissions should appear in the objective function, the new analytical approximation to the expected total emissions (in g) in the network during the simulation is given by,

$$E[E_{total}] = \sum_{\ell \in \mathcal{L}} y_{1\ell} E[T_\ell] \lambda_\ell \Delta T \tag{3.7}$$

3.4 Empirical Analysis

3.4.1 Experimental setup

The experimental setup used is identical to the one described in Section 2.4.1. We compare the performance of the methods Am, $A\phi$ and Ag^A for the objective function

$g^{T,EM}$ as defined in Equation (3.5). Once again, we consider different initial points, namely, an existing fixed-time signal plan for Lausanne city and randomly drawn feasible signal plans. We define the computational budgets for methods Am and $A\phi$ to be 150 simulation runs as before. The methods are compared based on the evaluation of the proposed signal plans when embedded within the Lausanne simulation model for a fixed number of replications set to 50 as before. We plot empirical cdf curves showing the performance of the signal plans proposed by each method on five different metrics, namely expected travel time in the network and expected total emissions of CO_2, NO_x, VOC and PM in the network.

3.4.2 Results

We perform a similar analysis as before (see Section 2.4.2) by comparing the performance of the signal plans derived by each algorithm in terms of different performance measures. Each figure in this section contains five cdf plots, one for each performance measure. Within each cdf plot there are 10 curves. The color coding of the curves is the same as before. There are four black curves, one for each of the signal plans proposed by the Am method. There are four red curves, one for each of the signal plans proposed by the $A\phi$ algorithm. There is one green curve for the signal plan proposed by the Ag^A algorithm and one blue curve for the initial signal plan.

In Figures 3-1 (a), (b), (c) and (d), the four best signal plans are proposed by Am. The signal plans proposed by Am also show reduced variability compared to those proposed by $A\phi$. One of the plans proposed by $A\phi$ does worse than the initial signal plan. In Figure 3-1(e), two of the signal plans proposed by $A\phi$ perform similarly to the ones proposed by Am while two do worse. The signal plan proposed by Ag^A performs worse than the initial signal plan for two performance metrics, namely NO_x and VOC emissions. In terms of travel time and CO_2 emissions, the Ag^A plan is able to achieve some improvement over the initial signal plan and in case of PM emissions, this plan achieves significant improvement over the initial signal plan. The trends seen on comparing the algorithms Am and $A\phi$ are consistent throughout the first four performance metrics (namely travel time, CO_2, NO_x and VOC) but change

when it comes to the fifth performance metric i.e. total PM emissions in the network.

Figure 3-2 considers a different random (uniformly drawn) initial signal plan. In Figure 3-2 (a)-(d), the three best signal plans are proposed by Am. Two of the signal plans proposed by $A\phi$ do worse than the initial signal plan. The degree of variability is also higher in the plans proposed by $A\phi$ than in those proposed by Am. The signal plan proposed by Ag^A is able to achieve improvements over the initial plan here but does worse than all four of the plans proposed by Am and two of the plans proposed by $A\phi$. In Figure 3-2(e), two of the three best plans are proposed by Am. One of the $A\phi$ plans and the plan proposed by Ag^A perform worse than the initial plan.

Figure 3-3 uses the existing signal plan of Lausanne as the initial signal plan. When comparing algorithms for the travel time, CO_2, NO_x and VOC performance metrics, we observe that the best signal plan in each case is that proposed by Am. For these four performance metrics, one of the signal plans proposed by $A\phi$ does significantly worse than the initial signal plan. The degree of variability in the plans proposed by $A\phi$ is also higher than those proposed by Am. In Figure 3-3(e), three of the signal plans proposed by $A\phi$ perform similarly to the four plans proposed by Am. For all five performance metrics, the performance of the signal plan proposed by the method Ag^A is very similar to that of the initial signal plan. Thus, the green curve is barely distinguishable in each cdf plot of this figure.

Figure 3-4 summarizes the information in Figures 3-1, 3-2 and 3-3. Each cdf plot contains two curves. The black curve consists of all the Am signal plans displayed in the previously mentioned figures (i.e. each black curve consists of 50x5x3 = 750 observations of the respective performance measure). Similarly, each red curve consists of all the $A\phi$ signal plans displayed in the previously mentioned figures for that specific performance measure. Figure 3-4 shows that the signal plans proposed by Am significantly outperform those proposed by $A\phi$ over four performance metrics namely, average network travel time and total network emissions of CO_2, NO_x and VOC. For the last performance metric (i.e. PM emissions), the Am plans perform better than the $A\phi$ plans. Thus, we see an added value of using a combination of simulated and analytic information to perform optimizations compared to using just

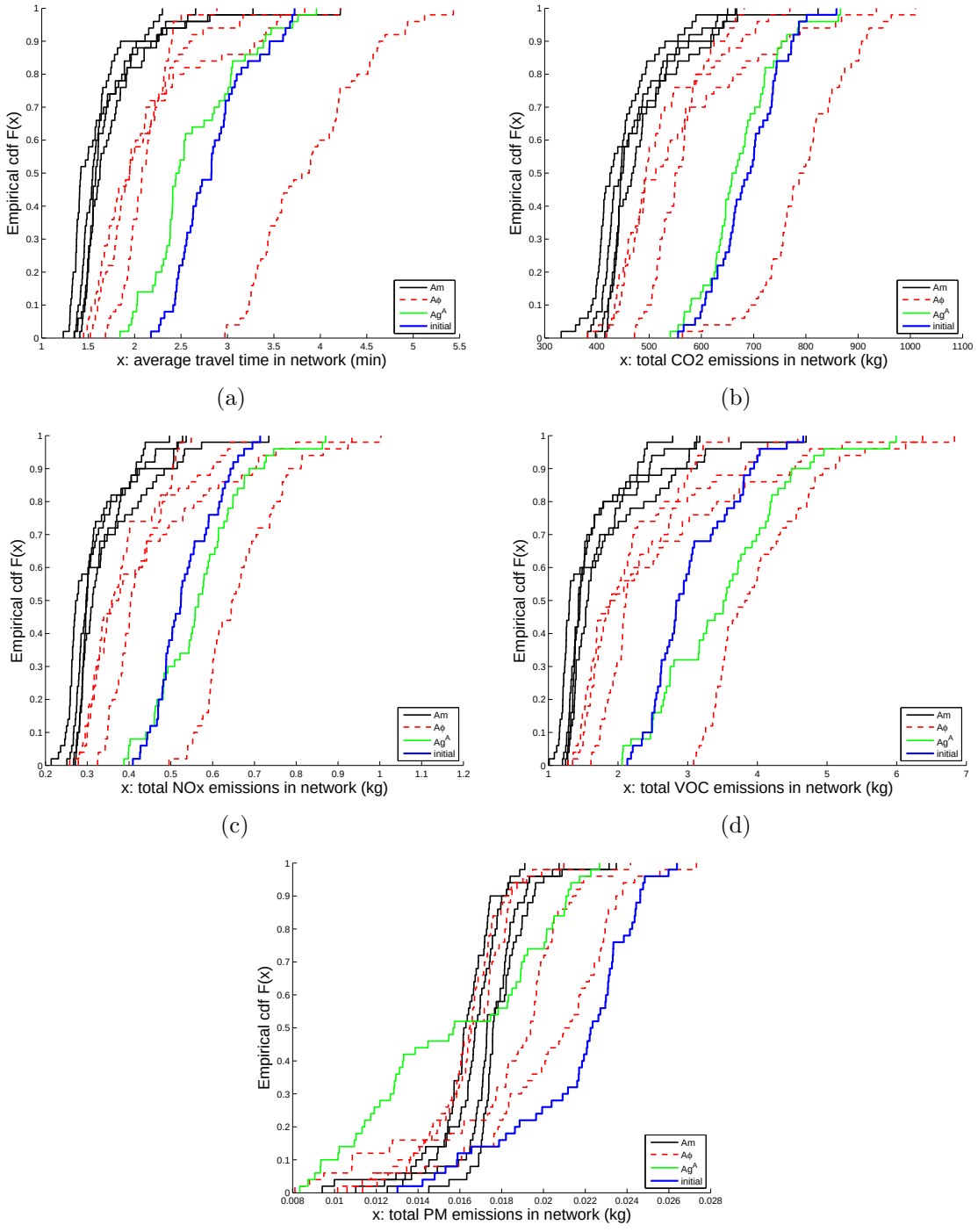

Figure 3-1: Performance of the signal plans derived with the $g^{T,EM}$ objective function and a random initial signal plan.

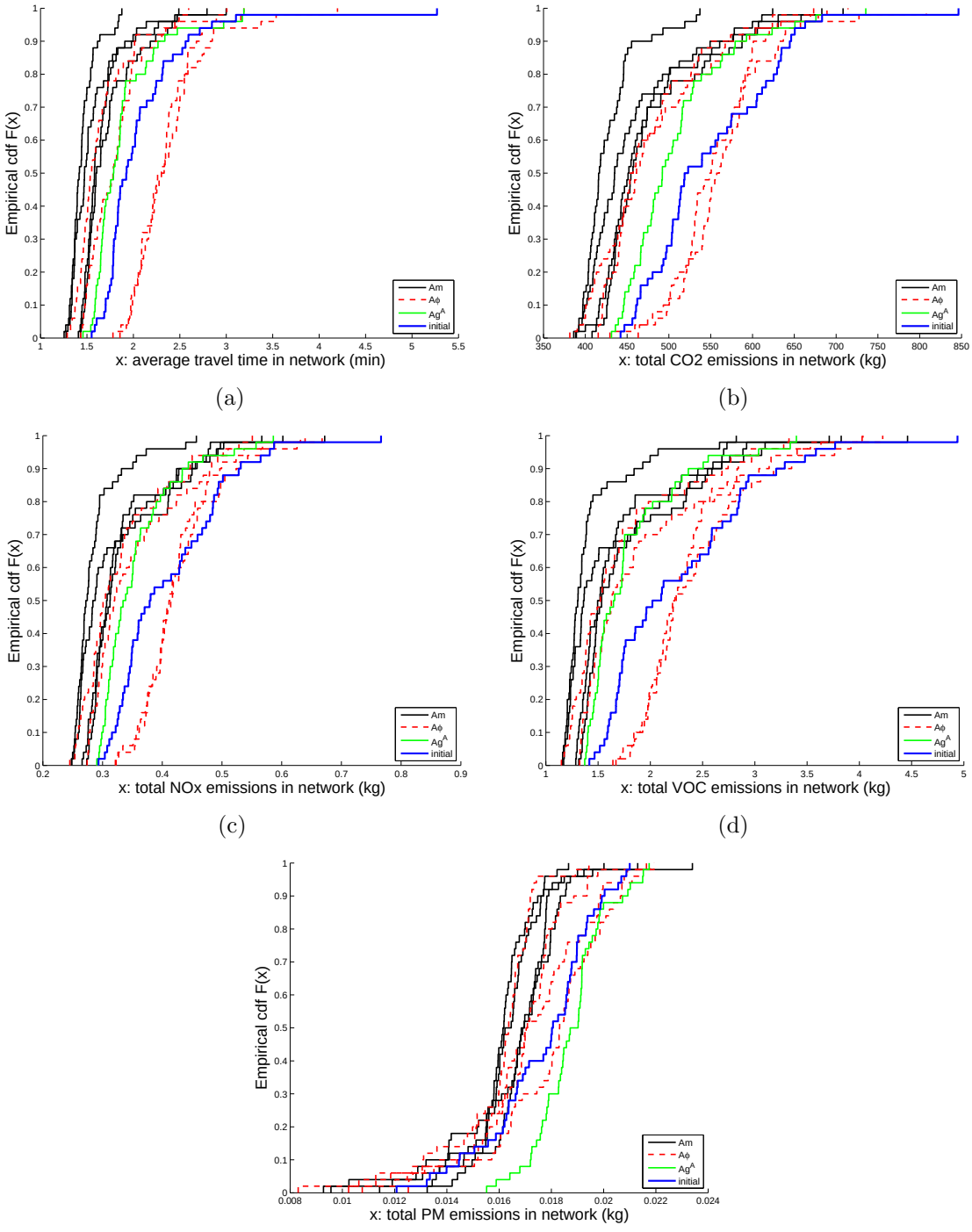

Figure 3-2: Performance of the signal plans derived with the $g^{T,EM}$ objective function and a random initial signal plan.

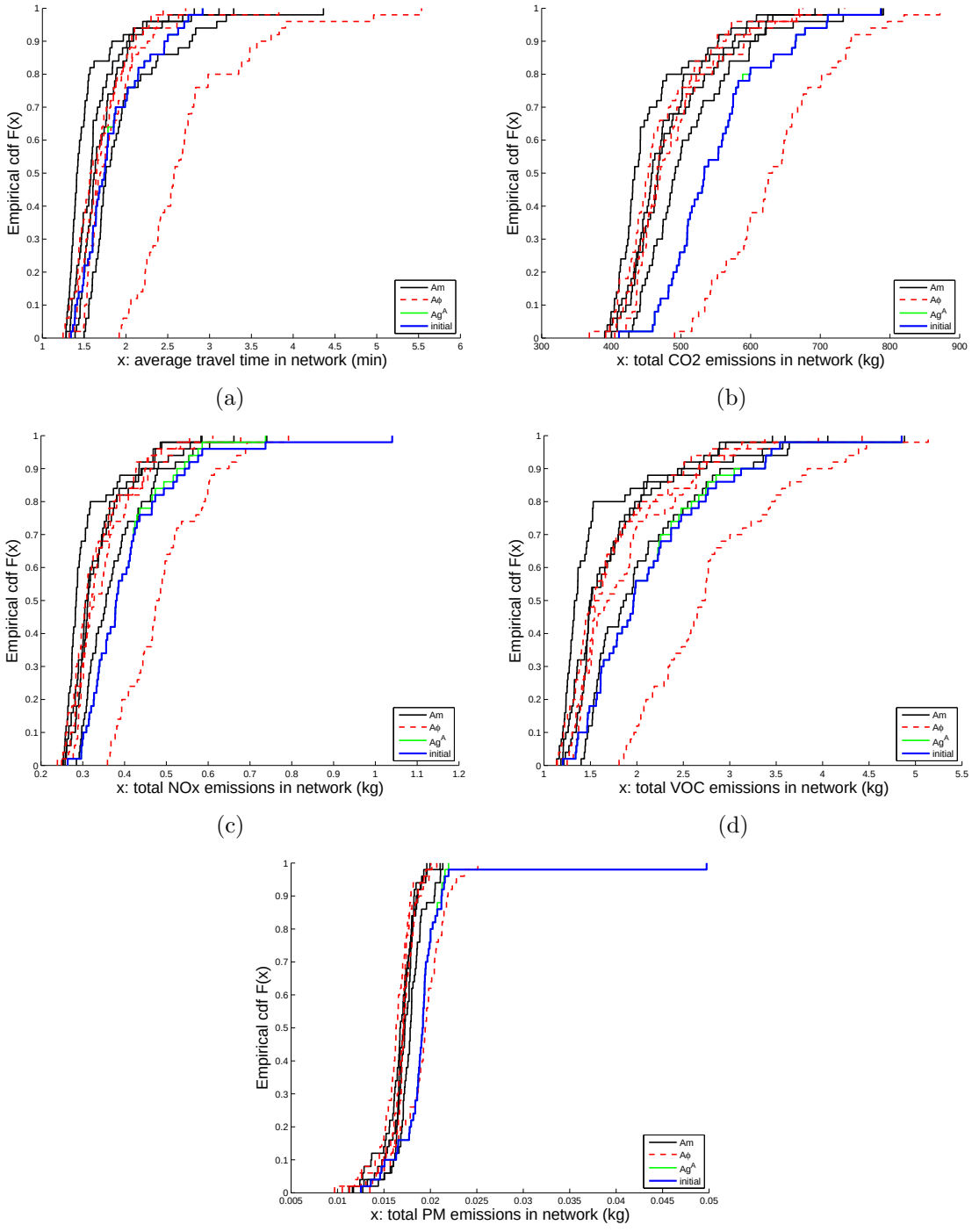

Figure 3-3: Performance of the signal plans derived with the $g^{T,EM}$ objective function. The algorithms are initialized with an existing signal plan for Lausanne.

simulated information. This once again can be attributed to the fact that emissions are dependent on individual vehicle attributes which show high variability from one simulation run to the next. Thus the use of an analytic emissions model in addition to the simulation model, makes the optimization process much more efficient.

Figure 3-5 considers the best signal plan proposed by the method Am when initialized with the existing signal plan of Lausanne city and demonstrates the monetary savings achieved when this plan is implemented during the one-hour evening peak period from 5 to 6 PM on a single day. In order to monetize the reduction in travel time and various pollutant emissions achieved by this plan for the considered network, we use the weights listed in Section 3.3. Figure 3-5 contains five cdf plots with two curves in each. The blue curve represents the externality costs for the existing signal configuration of Lausanne city and the black curve represents the externality costs when the best Am plan is implemented. The externality costs are given in EURO and are calculated for the one-hour evening peak period.

Figure 3-5 shows that the maximum cost savings are attributable to the reduction in network CO_2 levels followed next by the cost savings from reduction in total network travel time. The reduction in the externality costs of CO_2 emissions in the network ranges (across replications) from 200 to 700 EUROs. It is important to note that these savings are just for the evening peak period on a single day. Travel time savings for the network range (across replications) from zero to 300 EUROs.

Figure 3-6 shows the reduction in total externality cost, summed across travel time and all pollutant emissions in the network, achieved by the best Am plan over the initial signal plan.

Figures 3-7, 3-8, 3-9 and 3-10 consider the same initial point as Figure 3-1 and the objective function $g^{T,EM}$. Each plot displays the network of interest. Each link is colored according to the difference in the average (over 50 replications) emissions per vehicle between the best Am signal plan and the initial signal plan (i.e., positive values indicate a reduction in emissions achieved by the Am plan), for the pollutants CO_2, NO_x, VOC and PM, respectively. Links that are colored dark green see a significant reduction in emissions for that specific pollutant, while links colored light

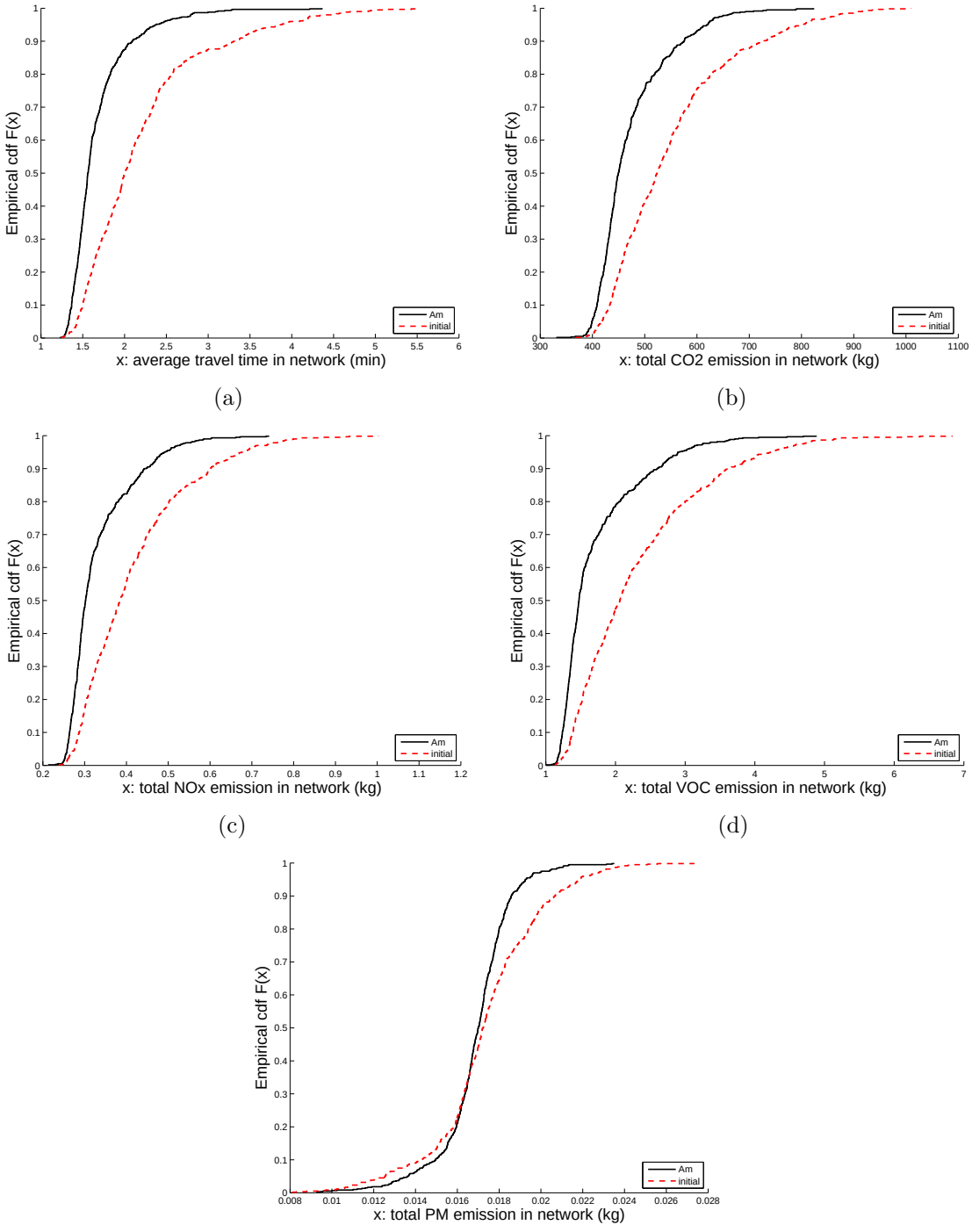

Figure 3-4: Summary of the performance of the signal plans derived with the $g^{T,EM}$ objective function.

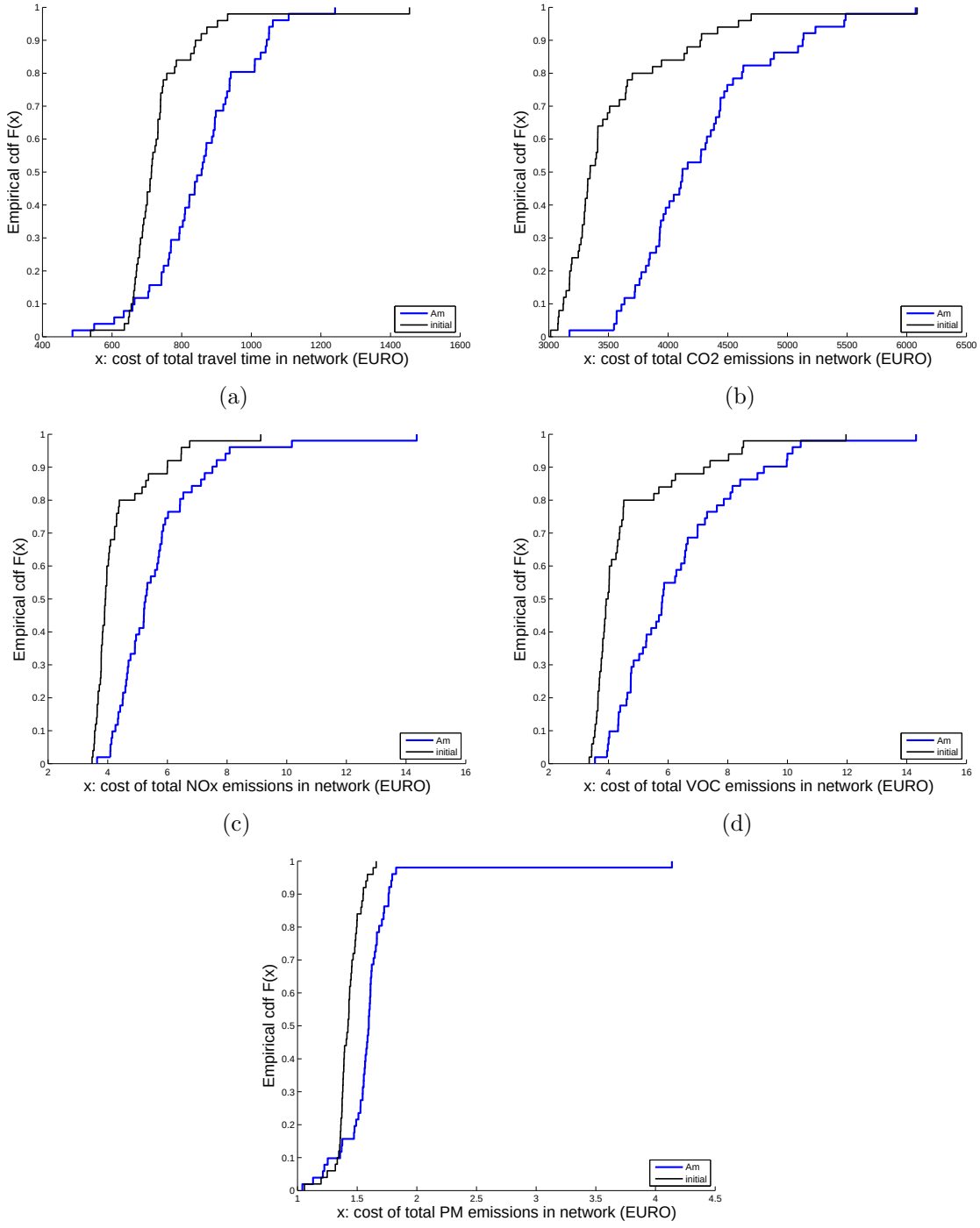

Figure 3-5: Monetary evaluation of the best signal plan proposed by *Am* when initialized with an existing signal plan for Lausanne.

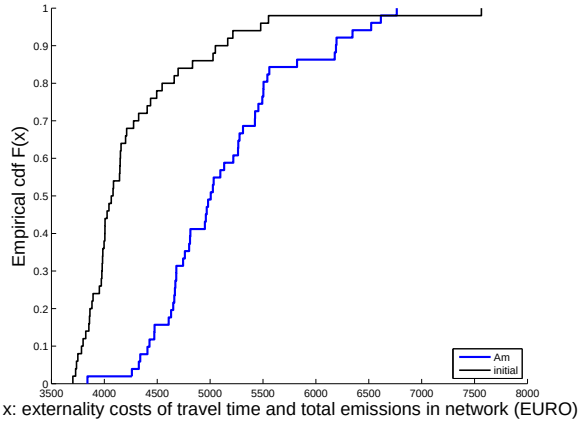

Figure 3-6: Monetary evaluation of the best signal plan proposed by *Am* in terms of total externality cost for the network

green see some reduction. Links colored orange see an increase in pollutant emissions for the *Am* plan compared to the initial plan and links colored red see a signficant increase. For each of the four pollutants, we see that the number of links showing a reduction in emissions for the *Am* plan is greater than the number of links showing an increase in emissions. The link-level emissions trends for the other random initial point (considered in Figure 3-2) are also similar and have not been displayed.

Figures 3-11, 3-12, 3-13 and 3-14 consider the existing signal plan of Lausanne as the initial signal plan. The coloring scheme is the same as for Figures 3-7 to 3-10 above. Here we see that the number of links for which the *Am* plan achieves a reduction in emission levels compared to the initial signal plan, is fewer than before. However, this number still exceeds the number of links which show an increase in emissions levels, for each of the four pollutant types.

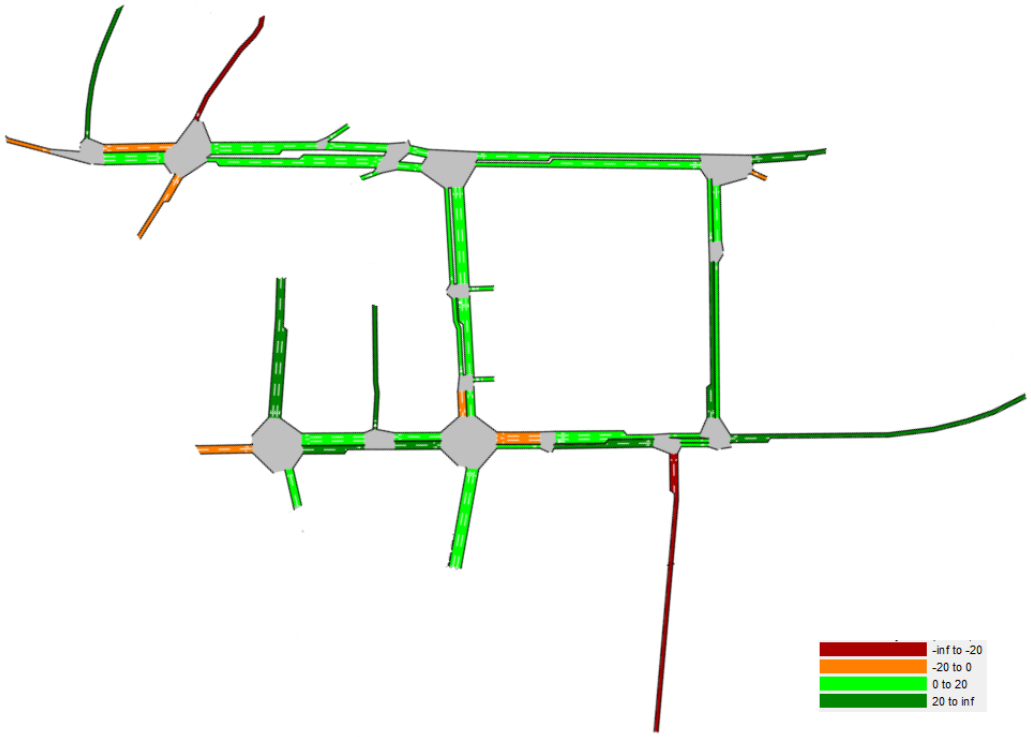

Figure 3-7: Improvement in average CO_2 emissions per vehicle per link (in g) achieved by the best *Am* plan when initialized with a random signal plan.

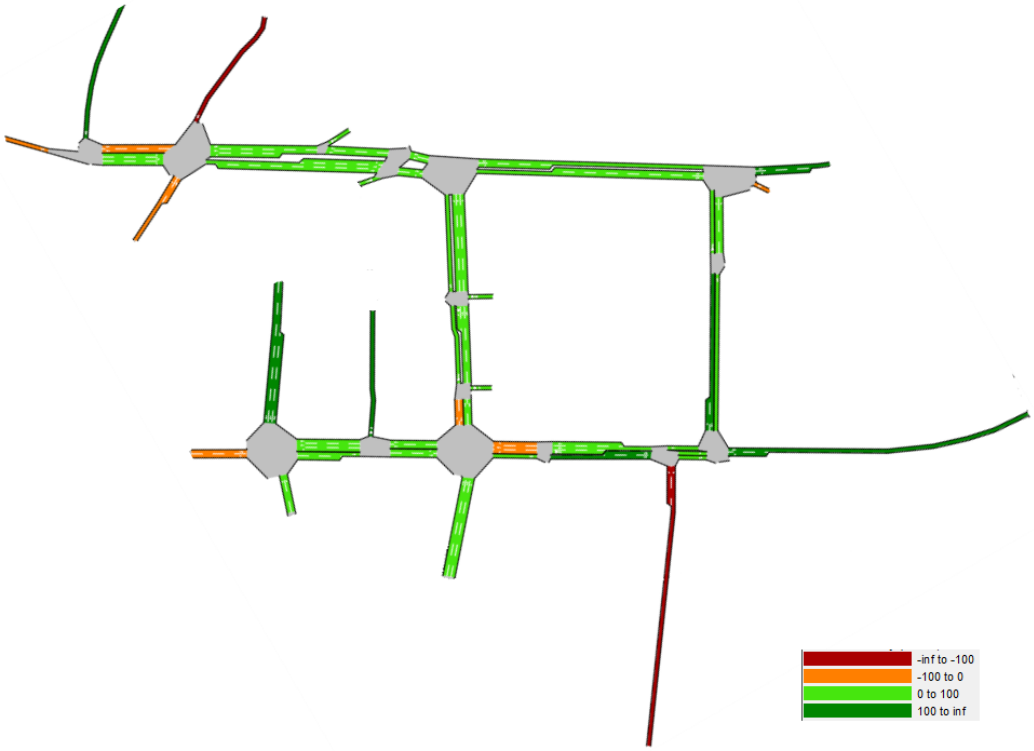

Figure 3-8: Improvement in average NO_x emissions per vehicle per link (in mg) achieved by the best *Am* plan when initialized with a random signal plan.

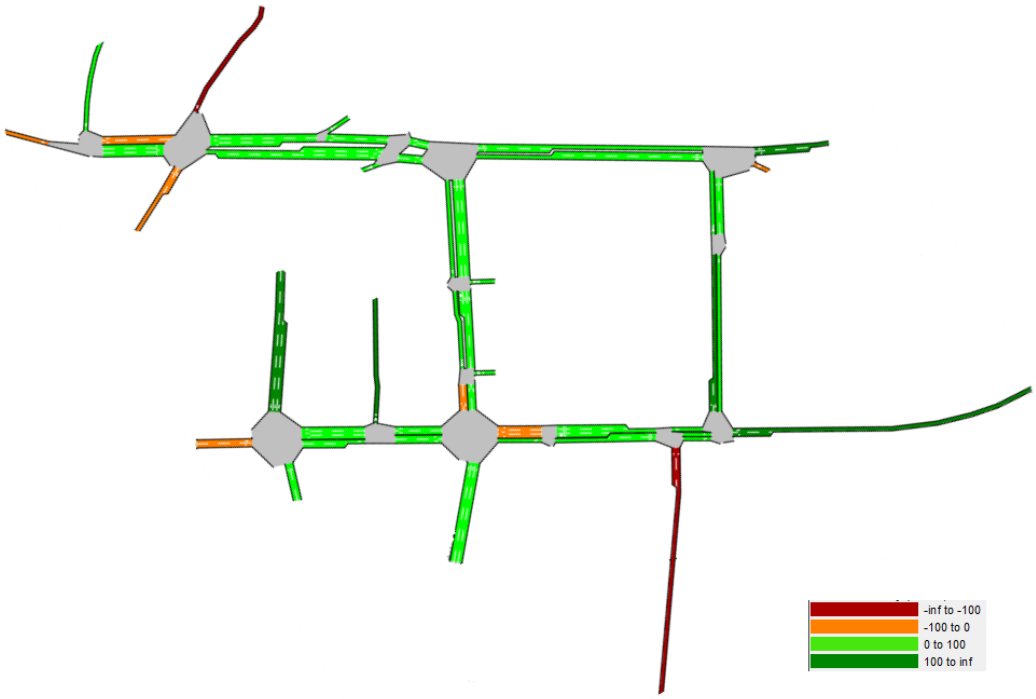

Figure 3-9: Improvement in average VOC emissions per vehicle per link (in mg) achieved by the best *Am* plan when initialized with a random signal plan.

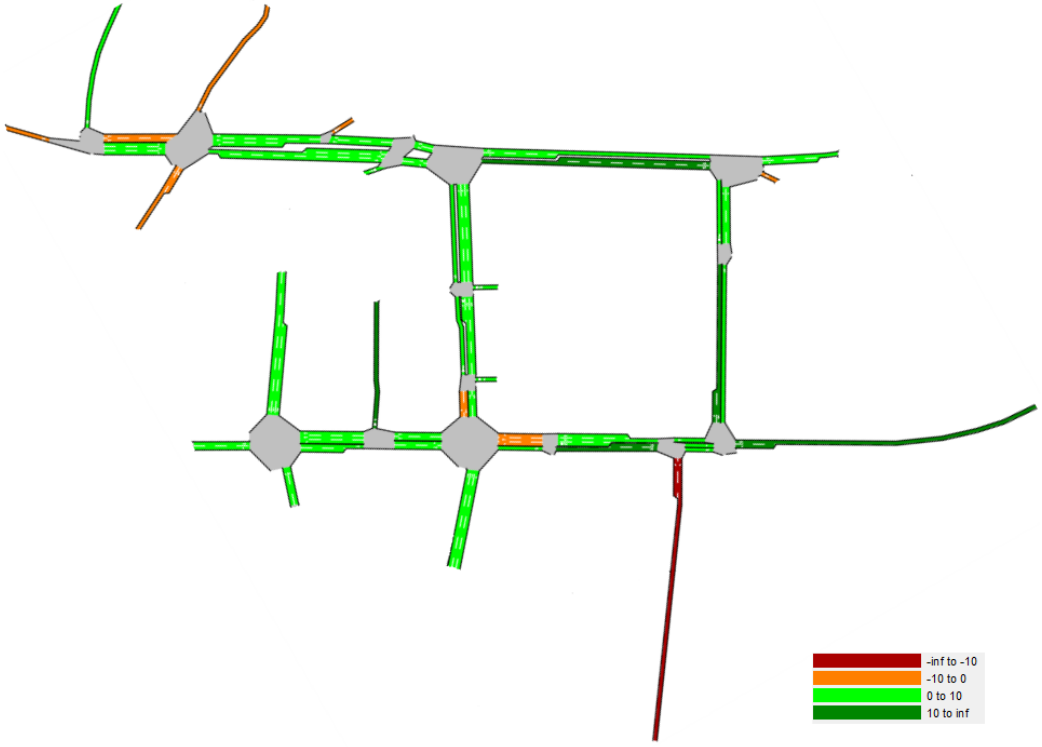

Figure 3-10: Improvement in average PM emissions per vehicle per link (in mg) achieved by the best *Am* plan when initialized with a random signal plan.

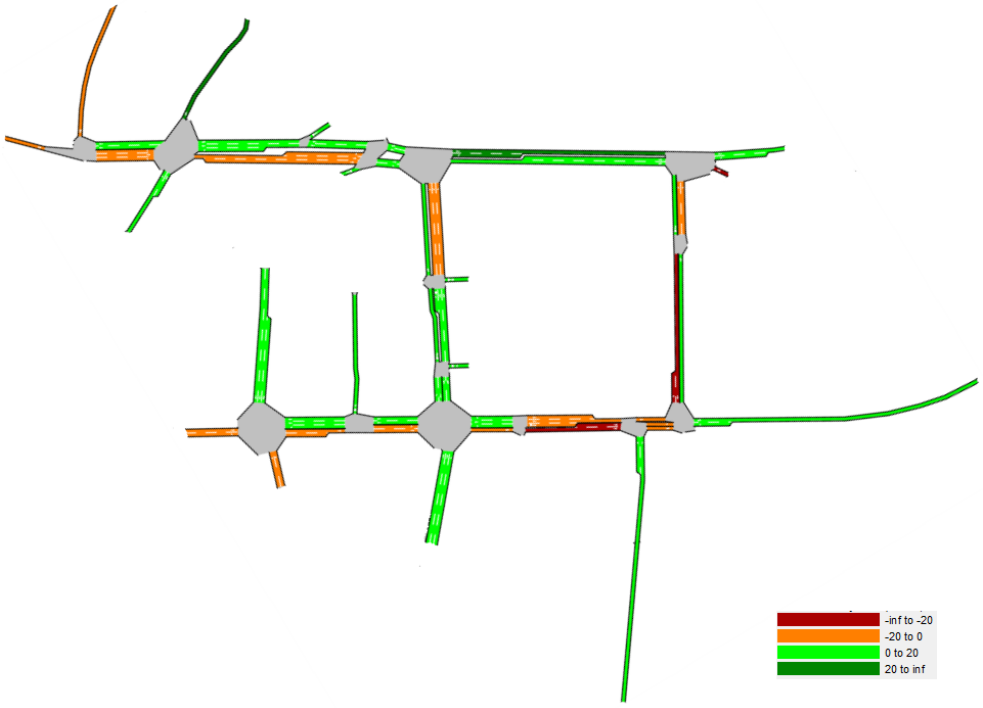

Figure 3-11: Improvement in average CO_2 emissions per vehicle per link (in g) achieved by the best *Am* plan when initialized with the existing signal plan of Lausanne.

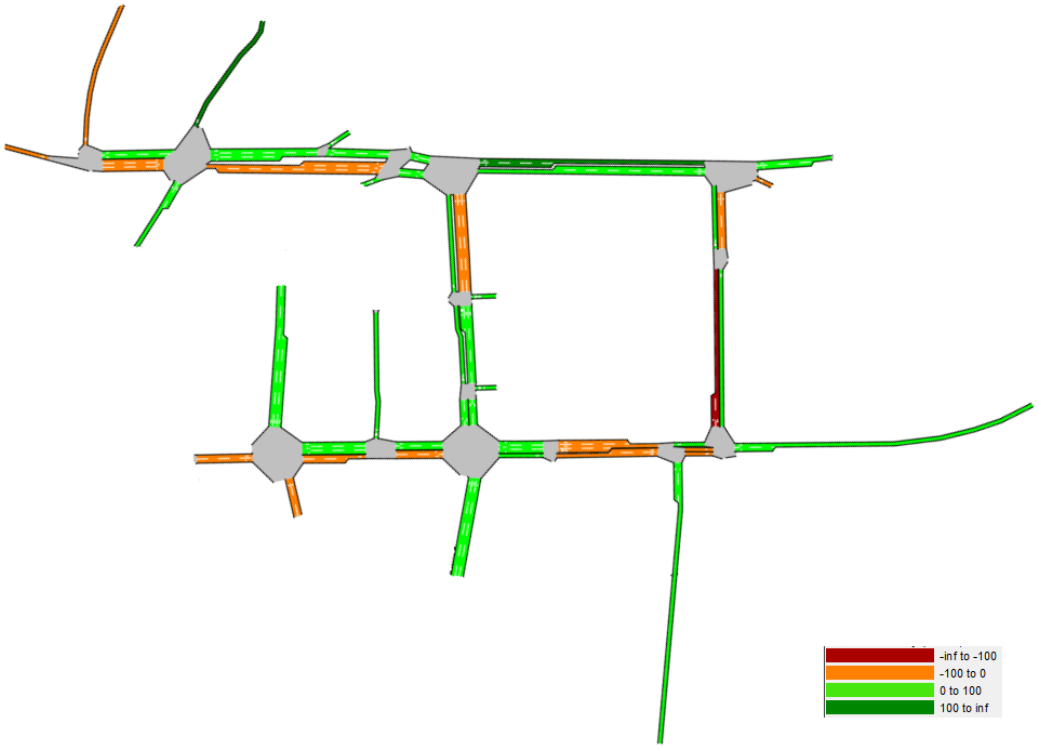

Figure 3-12: Improvement in average NO_x emissions per vehicle per link (in mg) achieved by the best *Am* plan when initialized with the existing signal plan of Lausanne.

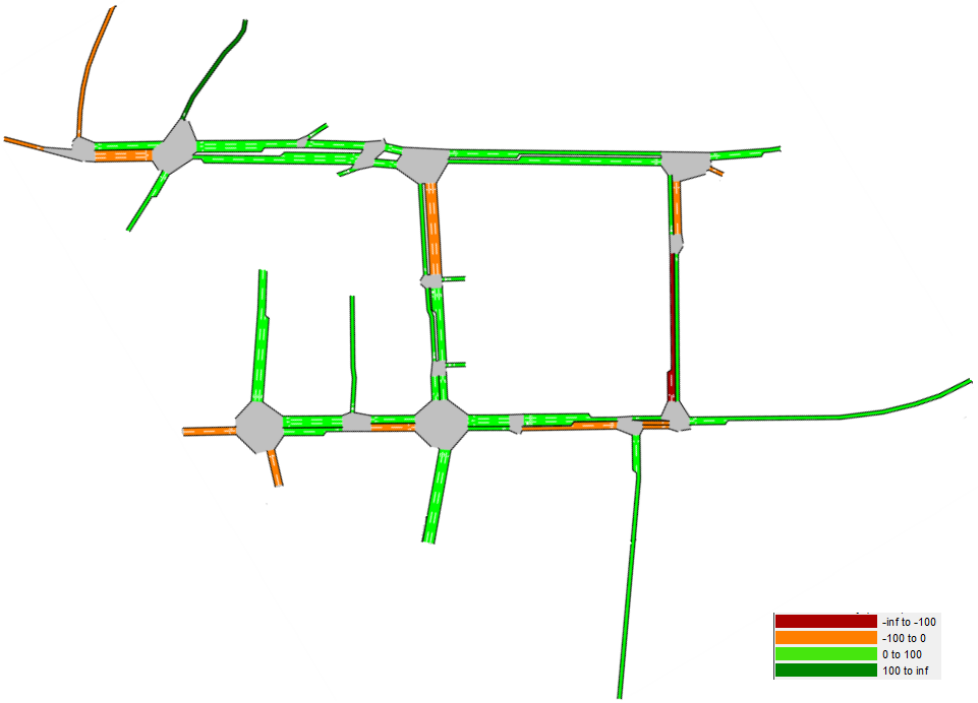

Figure 3-13: Improvement in average VOC emissions per vehicle per link (in mg) achieved by the best *Am* plan when initialized with the existing signal plan of Lausanne.

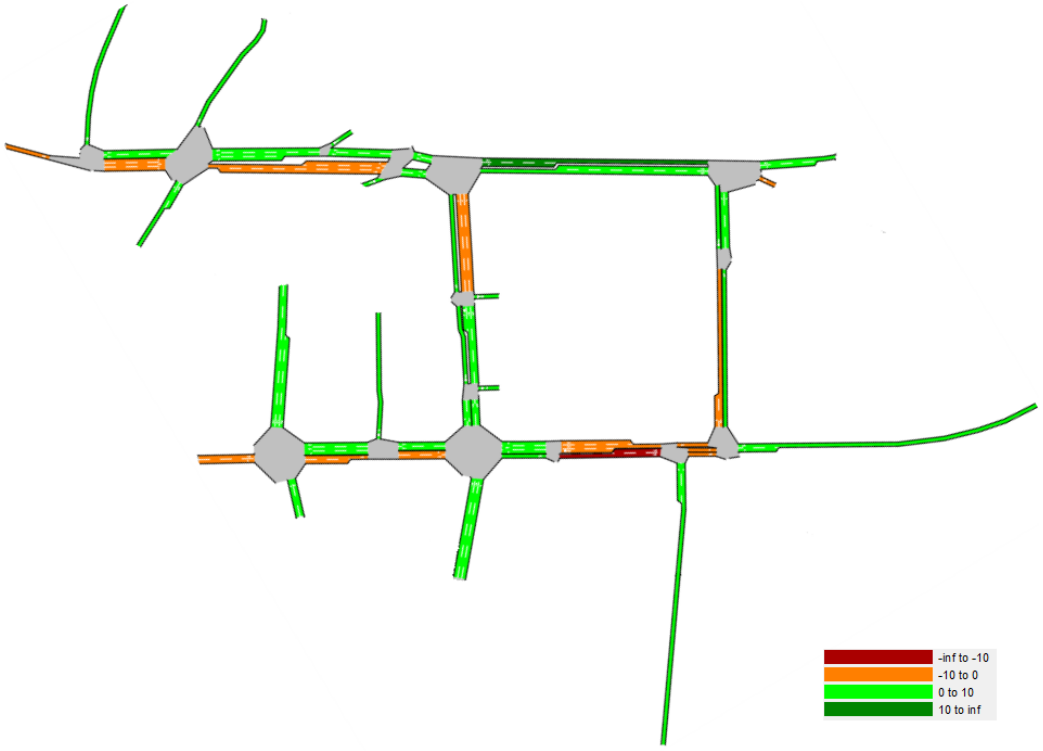

Figure 3-14: Improvement in average PM emissions per vehicle per link (in mg) achieved by the best *Am* plan when initialized with the existing signal plan of Lausanne.

3.4.3 Case study conclusions

The empirical analysis for a traffic network in the city of Lausanne presented in the Section 3.4.2 shows that there is an added value of combining simulated and analytical information. Since emissions of pollutants like CO_2, NO_x, VOC and PM depend strongly on individual vehicle attributes and complex local traffic dynamics, they have high variability. Thus, an algorithm which uses only simulated information is typically at a disadvantage compared to one that combines suitable analytical and simulated information. The analysis further details the monetary savings which can be achieved with the implementation of a signal plan derived using the proposed framework and demonstrates that the savings are significant. While the monetary savings are evaluated at the network-level, the empirical analysis also presents the reduction in emissions levels that are achieved at the link-level.

Chapter 4

Conclusions

The empirical case-studies of Chapter 2 and Chapter 3 show that when accounting for complex and high variance performance measures, such as fuel consumption and various pollutant emissions, there is an added value of combining information from the simulator with approximations derived from analytical macroscopic models. The proposed methodology outperforms both traditional methodologies: which resort to either only simulated information ($A\phi$) or only analytical information (Ag^A). The proposed methodology systematically achieves reductions in travel time, fuel consumption and emissions, and does so within a tight computational budget.

With energy efficiency and emissions mitigation being a growing concern for the transportation industry, this thesis demonstrates how detailed traffic and vehicle-performance simulation tools can be coupled and used to design traffic management strategies that improve network-wide performance metrics.

Ongoing work addresses optimization problems that account for environmental performance measures using signal control over a congested large-scale urban network. The addition of performance metrics with a high degree of variability in the objective function and the limited computational budget makes the development of an efficient framework a real challenge.

The importance of incorporating fuel consumption and emissions in a signal control framework is exemplified by, for instance, US federal regulations such as the Clean Air Act and the Surface Transportation Efficiency Act, which place increasing

responsibility on city and regional agencies to account for and achieve their environmental targets. By increasing accountability and using past performance as a metric for the procurement of future federal funding, these regulations also build incentive for governing agencies to conceive new insfrastructure schemes addressing sustainable transportation. The success of traffic management strategies is now dependent on their demonstrated ability to prevent further degradation of air quality in the surrounding areas while addressing city congestion. Signal control remains a low cost alternative in this regard. However, as is currently the practice, the use of integrated traffic-fuel-emissions models is primarily restricted to observing the effect of predetermined alternatives on emissions and/or fuel consumption. The optimization framework presented in this thesis enables practitioners to go beyond evaluation purposes and systematically identify alternatives with improved urban-scale performance. The tight computational budget also ensures that the time-span required to identify improved signal configurations is short.

While this domain has not been explored in the thesis, we believe that the combination of analytic and simulated information to address environmental objectives can be extended beyond signal control to include intelligent transportation system deployments, ramp metering and dynamic speed limits. Since the SO framework presented accounts for detailed vehicle-specific information, it can also be used to evaluate the performance of novel vehicle technologies, and to inform their design while accounting for the complex local interactions of drivers with both surrounding vehicles and with the underlying infrastructure.

Appendix A

Analytical queueing network model

The physical component of the metamodel is an analytical and differentiable urban traffic model. Each lane of an urban road network is modeled as a set of finite capacity queues. In the following notation the index i refers to a given queue. We refer the reader to Osorio and Bierlaire (2009b) and to Osorio and Bierlaire (2009a) for details.

γ_i	external arrival rate;
λ_i	total arrival rate;
μ_i	service rate;
$\tilde{\mu}_i$	unblocking rate;
μ_i^{eff}	effective service rate (accounts for both service and eventual blocking);
ρ_i	traffic intensity;
P_i^f	probability of being blocked at queue i;
k_i	upper bound of the queue length;
N_i	total number of vehicles in queue i;
$P(N_i = k_i)$	probability of queue i being full, also known as the blocking or spillback probability;
p_{ij}	transition probability from queue i to queue j;
$\mathscr{D}_i$	set of downstream queues of queue i;

The queueing network model is formulated as follows.

$$
\begin{cases}
\lambda_i = \gamma_i + \dfrac{\sum_j p_{ji}\lambda_j(1 - P(N_j = k_j))}{(1 - P(N_i = k_i))}, & \text{(A.1a)} \\
\dfrac{1}{\tilde{\mu}_i} = \displaystyle\sum_{j \in \mathscr{D}_i} \dfrac{\lambda_j(1 - P(N_j = k_j))}{\lambda_i(1 - P(N_i = k_i))\mu_j^{\text{eff}}}, & \text{(A.1b)} \\
\dfrac{1}{\mu_i^{\text{eff}}} = \dfrac{1}{\mu_i} + P_i^f \dfrac{1}{\tilde{\mu}_i}, & \text{(A.1c)} \\
P(N_i = k_i) = \dfrac{1 - \rho_i}{1 - \rho_i^{k_i+1}}\rho_i^{k_i}, & \text{(A.1d)} \\
P_i^f = \displaystyle\sum_j p_{ij} P(N_j = k_j), & \text{(A.1e)} \\
\rho_i = \dfrac{\lambda_i}{\mu_i^{\text{eff}}}, & \text{(A.1f)}
\end{cases}
$$

The exogenous parameters are γ_i, μ_i, p_{ij} and k_i. All other parameters are endogenous. When used to solve a signal control problem (as in this thesis), the capacity of the signalized lanes become endogenous, which makes the corresponding service rates, μ_i, endogenous.

Appendix B

Trust region subproblem

At a given iteration k, the SO algorithm considers a metamodel $m_k(x, y; \alpha_k, \beta_k, q)$, an iterate x_k (point considered to have best performance so far) and a trust region (TR) radius Δ_k, and solves the TR subproblem in order to derive a trial point (i.e., a signal plan with potentially improved performance). The TR subproblem is formulated as follows:

$$\min_{x,y} \; m_k = \alpha_k g^A(x, y; q) + \phi(x; \beta_k) \tag{B.1}$$

subject to

$$\sum_{j \in \mathscr{P}_I(i)} x(j) = b_i, \; \forall i \in \mathscr{I} \tag{B.2}$$

$$h(x, y; q) = 0 \tag{B.3}$$

$$\mu_\ell - \sum_{j \in \mathscr{P}_L(\ell)} x_j s = 0, \; \forall \ell \in \mathcal{L} \tag{B.4}$$

$$\|x - x_k\|_2 \leq \Delta_k \tag{B.5}$$

$$y \geq 0 \tag{B.6}$$

$$x \geq x_L, \tag{B.7}$$

where s denotes the saturation flow rate, $\mathcal{L}$ denotes the set of indices of the signalized lanes, $\mathscr{P}_L(\ell)$ denotes the set of phase indices of lane ℓ, and h is the analytical traffic model.

The TR subproblem differs from the signal control problem given in Section 2.3 (Equations (2.28), (2.29) and (2.30)) as follows. The TR subproblem approximates the objective functions by the metamodel at iteration k, m_k. It includes the following additional constraints:

- Inequality (B.5). This is known as the trust region constraint.
- Equation (B.3). The function h of Equation (B.3) represents the queueing network model given above by the System of Equations (A.1).
- Equation (B.4). This equation relates the green splits of a phase to the flow capacity of the underlying signalized lanes (i.e., the service rate of the queues).
- Equation (B.6). The endogenous variables of the queueing model are subject to positivity constraints.

Bibliography

Akçelik, R. (1983). Progress in fuel consumption modelling for urban traffic management, *Technical Report Research Report ARR 124*, Australian Road Research Board.

Algers, S., Bernauer, E., Boero, M., Breheret, L., Di Taranto, C., Dougherty, M., Fox, K. and Gabard, J.-F. (1997). Review of micro-simulation models, *Technical Report SMARTEST/D3*.

Bai, S., Chiu, Y.-C. and Niemeier, D. (2007). A comparative analysis of using trip-based versus link-based traffic data for regional mobile source emissions estimation, *Atmospheric Environment* **41**: 7512–7523.

Barceló, J. (2010). *Fundamentals of traffic simulation*, Vol. 145 of *International Series in Operations Research and Management Science*, Springer, New York, USA.

Bartin, B., Mudigonda, S. and Ozbay, K. (2007). Impact of electronic toll collection on air pollution levels: Estimation using microscopic simulation model of large-scale transportation network, *Transportation Research Record: Journal of the Transportation Research Board* **2011**(1): 68–77.

Bottom, J. (2000). *Consistent anticipatory route guidance*, PhD thesis, Massachusetts Institute of Technology.

Boxill, S. and Yu, L. (2000). An evaluation of traffic simulation models for supporting its development, *Technical Report 167602-1*, Texas Southern University.

Caliper (2008). *TransModeler 4.1 User's Guide*.

Cappiello, A. (2002). *Modeling traffic flow emissions*, Master's thesis, Massachusetts Institute of Technology, Cambridge, MA, USA.

CARB (2008). *EMFAC 1.0 User's Guide*, California Air Quality Research Board.

Chen, X., Osorio, C. and Santos, B. F. (2012). A simulation-based approach to reliable signal control, *Proceedings of the International Symposium on Transportation Network Reliability (INSTR)*.

Chiu, Y., Nava, E., Zheng, H. and Bustillos, B. (2011). *DynusT 3.0 User's Manual*.

Conn, A. R., Scheinberg, K. and Vicente, L. N. (2009). Global convergence of general derivative-free trust-region algorithms to first- and second-order critical points, *SIAM Journal on Optimization* **20**(1): 387–415.

Dumont, A. G. and Bert, E. (2006). Simulation de l'agglomération Lausannoise SIMLO, *Technical report*, Laboratoire des voies de circulation, ENAC, Ecole Polytechnique Fédérale de Lausanne.

EPA, U. (1994). *User's Guide to MOBILE5 (Mobile Source Emission Factor Model*, US Environmental Protection Agency.

EPA, U. (2003). *User's Guide to MOBILE6.1 and MOBILE6.2*, US Environmental Protection Agency.

EPA, U. (2010). *Motor Vehicle Emission Simulator (MOVES) User Guide*, US Environmental Protection Agency.

Ferreira, L. J. A. (1982). Car fuel consumption in urban traffic. the results of a survey in Leeds using instrumented vehicles, *Technical Report 162*, Institute for Transportation Studies. University of Leeds.

IEA (2012). Technology roadmap. fuel economy of road vehicles, *Technical report*, International Energy Agency.

Ikeda, R., Kawashim, H. and Oda, T. (1999). Determination of traffic signal settings for minimizing fuel consumption, *Intelligent Transportation Systems, IEEE*, pp. 272–277.

Lee, G., You, S. I., Ritchie, S. G., Saphores, J.-D., Sangkapichai, M. and Jayakrishnan, R. (2009). Environmental impacts of a major freight corridor, *Transportation Research Record: Journal of the Transportation Research Board* **2123**(1): 119–128.

Li, X. (1999). *The GIS Based Simulation on Emission Pollution from Urban Traffic*, PhD thesis, Southeast University.

Li, X., Li, G., Pang, S., Yang, X. and Tian, J. (2004). Signal timing of intersections using integrated optimization of traffic quality, emissions and fuel consumption, *Transportation Research Part D* **9**(5): 401–407.

Liao, T. and Machemehl, R. B. (1998). Fuel consumption estimation and optimal traffic signal timing, *Technical Report SWUTC/98/467312-1*, Southwest Region University Transportation Center, Center for Transportation Research, University of Texas at Austin.

Lin, J., Chiu, Y., Vallamsundar, S. and Bai, S. (2011). Integration of moves and dynamic traffic assignment models for fine-grained transportation and air quality analyses, *IEEE Forum on Integrated and Sustainable Transportation System (FISTS),Vienna,Austria*, IEEE, pp. 176–181.

Little, J. D. C. (1961). A proof for the queuing formula: L= λ W, *Operations Research* **9**(3): 383–387.

Liu, R. (2005). *DRACULA 2.3 User Manual*, Institute for Transport Studies, University of Leeds, UK. Available at http://www.its.leeds.ac.uk/software/dracula/tnote2.pdf (Last accessed on May 17, 11:20 PM).

Liu, R. and Tate, J. (2000). Microsimulation modeling of intelligent speed adaptation systems, *European Transport Conference, Seminar J, Cambridge, UK*, number 89-100.

Madireddy, M., De Coensel, B., Can, A., Degraeuwe, B., Beusen, B., De Vlieger, I. and Botteldooren, D. (2011). Assessment of the impact of speed limit reduction and traffic signal coordination on vehicle emissions using an integrated approach, *Transportation research part D: transport and environment* **16**(7): 504–508.

Mahmassani, H., Sbayti, H. and Zhou, X. (2004). *DYNASMART-P Version 930.9 User's Guide*.

Mayeres, I., Ochelen, S. and Proost, S. (1996). The marginal external costs of urban transport, *Transportation Research Part D* **1**(2): 111–130.

Messmer, A. and Papageorgiou, M. (1990). Metanet: A macroscopic simulation program for motorway networks, *Traffic Engineering and Control* **31**: 466–477.

Osorio, C. (2010). *Mitigating network congestion: analytical models, optimization methods and their applications*, PhD thesis, Ecole Polytechnique Fédérale de Lausanne.

Osorio, C. and Bierlaire, M. (2009a). An analytic finite capacity queueing network model capturing the propagation of congestion and blocking, *European Journal of Operational Research* **196**(3): 996–1007.

Osorio, C. and Bierlaire, M. (2009b). A surrogate model for traffic optimization of congested networks: an analytic queueing network approach, *Technical Report 090825*, Transport and Mobility Laboratory, ENAC, Ecole Polytechnique Fédérale de Lausanne.

Osorio, C. and Bierlaire, M. (2010). A simulation-based optimization approach to perform urban traffic control, *Proceedings of the Triennial Symposium on Transportation Analysis (TRISTAN)*, Tromsø, Norway. Submitted for publication.

Osorio, C. and Chong, L. (2012). Large-scale simulation-based traffic signal control, *International Symposium on Dynamic Traffic Assignment (DTA)*, Martha's Vineyard, USA.

Osorio, C. and Nanduri, K. (2012). Energy-efficient traffic management: a microscopic simulation-based approach, *International Symposium on Dynamic Traffic Assignment (DTA)*, Martha's Vineyard, USA.

Panis, L., Broekx, S. and Liu, R. (2006). Modeling instantaneous traffic emission and the influence of traffic speed limits, *Science of the Total Environment* **371**: 270–285.

PTV (2008). *VISSIM 4.30 User's Manual*, Planung Transport Verkehr AG, Karlsruhe, Germany.

Quadstone (2009). *PARAMICS v5.0 Modeller Reference Manual*.

QUARTET (1992). *Assessment of current tools for environment assessment in QUARTET, Drive II Project V2018*.

Rakha, H., Ahn, K. and Trani, A. (2003). Comparison of mobile5a, mobile6, vt-micro and cmem models for estimating hot-stabilized light-duty vehicle emissions, *Canadian Journal of Civil Engineering* **30**(6): 1010–1021.

Rakha, H., Ahn, K. and Trani, A. (2004). Development of VT-Micro model for estimating hot stabilized light duty vehicle and truck emissions, *Transportation Research Part D* **9**(1): 49–74.

Rakha, H., Van Aerde, M., Ahn, K. and Trani, A. (2000). Requirements for evaluating traffic signal control impacts on energy and emissions based on instantaneous speed and acceleration measurements, *Transportation Research Board Annual Meeting*, Washington DC, USA.

Robertson, D. I. (1969). TRANSYT - a traffic network study tool, *Technical Report LR 253*, Transport and Road Research Laboratory TRRL.

Robertson, D. I. (1983). Coordinating traffic signals to reduce fuel consumption, *Proceedings of the Royal Society of London. Series A, Mathematical and Physical Sciences* **387**(1792).

Scora, G. and Barth, M. (2006). *Comprehensive Modal Emission Model (CMEM) Version 3.01 User's Guide*, University of California, Riverside.

Smit, R., Smokers, R. and Rabe, E. (2007). A new modeling approach for road traffic emissions, *Transportation Research Part D* **12**: 414–422.

Stafford, R. (2006). *The Theory Behind the 'randfixedsum' Function*. http://www.mathworks.com/matlabcentral/fileexchange/9700.

Stathopoulos, F. G. and Noland, R. B. (2003). Induced travel and emissions from traffic flow improvement projects, *Transportation Research Record* **1842**: 57–63.

Stevanovic, A., Stevanovic, J., Zhang, K. and Batterman, S. (2009). Optimizing traffic control to reduce fuel consumption and vehicular emissions. integrated approach with VISSIM, CMEM, and VISGAOST, *Transportation Research Record* **2128**: 105–113.

Stevanovic, J., Stevanovic, A., Martin, P. T. and Bauer, T. (2008). Stochastic optimization of traffic control and transit priority settings in VISSIM, *Transportation Research Part C* **16**(3): 332 – 349.

Tijms, H. C. (2003). *A First Course in Stochastic Models*, Wiley, Chichester, West Sussex, England.

TSS (2011). *AIMSUN 6.1 Microsimulator Users Manual*, Transport Simulation Systems.

UK DOT (1994). *New Car Fuel Consumption: the official figures*, UK Department of Transportation. As cited in the 2011 AIMSUN 6.1 Microsimulator Users Manual.

Van Aerde, M. (1999). *INTEGRATION Release 2.20 User's Guide*, Van Aerde and Assoicates.

VSS (1992). *Norme Suisse SN 640837 Installations de feux de circulation; temps transitoires et temps minimaux*, Union des professionnels suisses de la route, VSS, Zurich.

WHO and GIZ (2011). Urban transport and health, module 5g, *Technical report*, World Health Organization and Transport Policy Advisory Services (GIZ).

Williams, L. and Yu, L. (2001). A conceptual examination of the impact of traffic control strategies on vehicle emission and fuel consumption, *Technical Report SWUTC/01/467203*, Texas Southern University.

Xiang, Q. (2000). *Analyzing the Fuel Consumption of Urban Traffic Systems*, PhD thesis, Southeast University.

Xie, Y., Chowdhury, M., Bhavsar, P. and Zhou, Y. (2011). An integrated tool for modeling the impact of alternative fueled vehicles on traffic emissions: A case study of greenville, south carolina, *Transportation Research Board 90th Annual Meeting*, number 11-3880.

Yu, L. (1994). A mathematical programming based approach to macroscopic traffic assignment in a dynamic network with queues, *Technical report*, Department of Civil Engineering, Queen's University.

Zegeye, S., Schutter, B., Hellendoorn, H. and Breunesse, E. (2010). Model-based traffic control for balanced reduction of fuel consumption, emissions and travel time, *Proceedings of the 12th IFAC Symposium on Transportation Systems*, Redondo Beach, CA, USA.